Dmo2p is required for Cox2p stability and plays a role in mitochondrial redox balance.

Maria Antônia Kfouri Martins Soares[1], Leticia Veloso Ribeiro Franco[1], Jhulia Almeida Clarck Chagas[1], Fernando Gomes[2], Mário H. Barros[1]

1- Departamento Microbiologia- Instituto Ciências Biomédicas - Universidade de São Paulo – São Paulo, Brazil
2- Departamento Biologia-Genética – Instituto Biociências – Universidade de São Paulo – São Paulo, Brazil

Correspondence address: Mario H. Barros, Departamento de Microbiologia, Instituto de Ciências Biomédicas, Universidade de São Paulo, Av. Professor Lineu Prestes, 1374, 05508-900, São Paulo, Brazil; email: mariohb@usp.br

Running Title – Dmo2 putative moonlight protein involved in copper trafficking and redox control.

Keywords: COX assembly, CuA site formation, DMAC1 homolog

Abstract

Although *Saccharomyces cerevisiae* multi-omic studies have unveiled the function of many proteins, several with elusive functions remain to be fully understood. Based on available platforms of mitochondrial proteome and expression studies, we selected the yeast ORF *YDL157c* for further characterization. In the meantime, the same ORF was identified by other groups using a machine learning approach as required for mitochondrial translation and it was renamed as *DMO2*. Dmo2p is a homolog to human DMAC1; it contains conserved cysteines in a Cx_2C motif and was previously detected in the peroxisome and in the mitochondrial proteome. Our work discloses Dmo2p as a new factor required for the stabilization of a newly translated mitochondrial product Cox2p, the subunit two of the cytochrome *c* oxidase complex. Three pieces of evidence have led us to this conclusion: first, elevated instability of newly translated Cox2p in the *dmo2* null mutant; second, Dmo2p pulled down components of Cox2p maturation and metalation processes such as Sco1p, Sco2p, and Cox2p itself; and third, expression of *DMO2* in multicopy plasmids led to phenotypic suppression of the *cox23* mutant that has impaired copper traffic to COX metalation. Moreover, we also observed several phenotypes in *dmo2* mutants that indicate a general function of Dmo2p in cellular stress response; the null mutant did not grow on oleate medium, it is more sensitive to heat and oxidative stress, while its overexpression confers resistance to the tested oxidants.

Introduction

Saccharomyces cerevisiae genomic era started in 1996 with the completion of its genome and the realization that we did not know much about the function of roughly 3000 genes of this yeast (Goffeau et al., 1996). Ten years after this yeast genome sequencing, and thousands of articles published, there were more than one thousand uncharacterized genes (Peña-Castillo and Hughes, 2007); fifteen years more in this timeline and there is still a long way to go; indeed, slow progress in defining the function of the last twenty percent of genes is similar in different eukaryotes (Wood et al., 2019). Multi-omics approaches have been developed to accelerate this process providing useful insights into their function with the combination of modern large-scale and classical reductionist approaches (Sung et al., 2020; Stefely et al., 2016). We took advantage of the y3k project (Stefely et al., 2016) and thecellmap.org (Usaj et al., 2017) to select uncharacterized genes that may be involved in yeast mitochondrial respiration. Here we detail the involvement of poorly characterized protein Dmo2p in Cox2p stability, a mitochondrially encoded subunit of cytochrome *c* oxidase. *DMO2* has a homolog in humans, DMAC1 involved in the assembly of the distal portion of the complex I membrane arm, which is required for supercomplex formation (Stroud et al., 2016).

Cytochrome *c* oxidase (COX) is the last enzyme acceptor of electrons in the mitochondrial respiratory chain. The COX holoenzyme in yeast comprises eleven subunits, with the catalytic core formed by the Cox1p, Cox2p, and Cox3p subunits encoded by mtDNA, while the other eight subunits are nuclearly encoded. The expression, processing and module formation of mitochondrially encoded subunits involve a complex interplay of multiple mitochondrial multifunctional proteins. These proteins are involved in diverse

steps, including chaperone-mediated folding, cleavage, heme *a* synthesis, heme *a*, and copper transport and insertion, and stabilization of the COX assembly modules (Franco et al., 2020; Barros and McStay, 2020). Studies on Cox2p expression, processing and maturation have led to the discovery of several factors directly involved in this process (Fox, 2012; Jett and Leary, 2017).

In yeast, *COX2* mRNA translation depends on Pet111p activation (Mulero and Fox, 1993; Green-Wilms, et al., 2001; Fiori et al., 2005). Newly translated Cox2p membrane insertion occurs in two steps and depends on transmembrane translocation performed by Oxa1p and Cox18p (He and Fox, 1997; Hell et al., 1998; Fiumera et al., 2007), and it is assisted by Mba1p (Lorenzi et al., 2016), Cox20p (Hell et al., 2000; Fiumera et al., 2009; Eliot et al, 2012), Pnt1p and Mss2p (He and Fox, 1999; Broadley et al., 2001; Saracco and Fox, 2002). Cox20p also stabilizes and chaperones the newly translated Cox2p protecting it from degradation (Eliot et al., 2012). The CuA site of Cox2p receives the metal groups from the metalochaperones Sco1p and Sco2p after Cox18p displacement, a process also intermediated by Cox20p (Bourens et al., 2014; Bourens and Barrientos, 2017). The trafficking of copper from the cytosol to mitochondria is still elusive, early studies proposed that Cox17p, Cox19p and Cox23p facilitate the transfer of copper ions from the cytosol to the IMS (Glerum et al., 1996b; Nobrega et al., 2002, Barros et al., 2004), however a non-proteinaceous copper ligand in the matrix was shown to be the copper source for metalation of COX (Cobine et al., 2006). At any rate, once in the intermembrane space, copper ions are transferred to Sco1p and Sco2p (Glerum et al., 1996a; Banci et al., 2008). Sco1p acts as a scaffold protein, altering the oxidation state of the cysteine ligands in Cox2p (Chinenov, 2000) and facilitating the ligation of copper ions into Cox2p CuA site. The yeast paralog Sco2p is not required for COX assembly but may regulate copper efflux

and stress (Leary et al., 2007) or have an overlapping role with Coa6p, an additional factor that is also required for the efficient formation of respiratory supercomplexes (Ghosh et al., 2016). Interestingly, newly synthesized Cox2p does not form complexes with any structural subunits until the Cox1p and Cox2p assembly modules associate. Indeed, Cox2p assembly intermediates were mainly found interacting with Cox18p and Cox20p, and a small fraction with Sco1p and Coa6p (Franco et al., 2018). Cox16p has been detected in both Cox1p and Sco2p-Cox2p assembly complexes and has been proposed to be the assembly factor involved in the association of Cox1p and Cox2p assembly modules (Aich et al., 2018; Cerqua et al., 2018; Su and Tzagoloff, 2017).

In this study, we identified Dmo2p as a new factor required for Cox2p stabilization. In the *dmo2* mutant, a greater instability of newly translated Cox2p was noted, which was also observed when other components of the Cox2p maturation process, such as *cox18*, *cox20*, *imp2*, and *sco2*, were absent. Moreover, the expression of *DMO2* in multicopy plasmids led to phenotypic suppression of the *cox23* mutant; the Cox23p gene product is also involved in copper trafficking (Barros et al., 2004). Previously, Dmo2p was shown to be associated with the peroxisomal membrane (Yifrach et al., 2022) and existing in the mitochondrial proteome (Reinders et al., 2006). This dual localization is often found in proteins with more than one function, also known as moonlight proteins (Jeffrey, 2018); in this work, we confirmed the mitochondrial localization and showed that Dmo2p is also required for heat and redox stress responses. Altogether, our data supports the hypothesis that Dmo2p can be classified as a moonlight protein (Gancedo and Flores, 2008).

Results

DMO2 overexpression and null mutant phenotypes.

We utilized available information from the y3k project (Stefely et al., 2016) and thecellmap.org (Usaj et al., 2017) to select uncharacterized genes with omic profiles similar to those of well-characterized mitochondrial proteins. Among the considered candidates, ORF *YDL157c* appeared to be an interesting target for further study in both databases. In the y3kproject, the *ydl157* mutant showed significantly lower abundance of proteins required for the OXPHOS system including Cox13p, Cox2p, Qcr8p and Atp20p (y3k. project.org screenshot Figure S1A). Additionally, respiratory mutants such as *mrp10, shy1*, and *atp12* displayed reduced abundance of the Ydl157c protein (Figure S1B). Furthermore, the *ydl157c* null mutant proteome, and metabolome, correlated with *mef2*, *mrpl11*, *mrp10* mutants, all of which are involved in mitochondrial translation (Figure S1C, S1D). The genetic profile of the *ydl157c* mutant exhibited correlations with mutants encoding mitochondrial proteins and demonstrated genetic negative interaction with several mitochondrial mutants (thecellmap.org screenshot Figure S2A and S2B). Our data mining work was later confirmed by a machine learning multi-omic integration study, which renamed *YDL157c* to *DMO2* and described its involvement in mitochondrial translation (Dickinson et al., 2022).

Deletion of *DMO2* in the BY4742 background led to respiratory growth restriction at 37°C, while in the W303-1A background, the growth restriction was less pronounced (Figure 1A). These differences in respiratory phenotypes between the two backgrounds can be attributed to the presence of a *hap1* mutant allele in BY4742, which affects the expression of several genes involved in mitochondrial biogenesis (Gaisne et al., 1999). To gather additional phenotypic information about *DMO2*, we challenged mutants and overexpressing strains with high-temperature exposure, oxidants, and metals. Since the assembly of the OXPHOS complexes relies on a balanced stoichiometry of their subunits,

an excess of processing factors can be detrimental to mitochondria. Previously, we screened the effects of overexpressed genes of the mitochondrial gene expression system, some of which led to increased loss of mtDNA (Gomes et al., 2013; Chagas et al., 2022). Here, we also observed that the W303-1A strain expressing a *GAL10-DMO2* construct led to approximately 50% of petite colonies formation after an overnight culture growth in galactose, indicating its toxicity (Figure 1B). To gather further phenotypic information about *DMO2*, we challenged mutants and overexpressing strains with high-temperature exposure, oxidants, and metals. In contrast, the *GPD-DMO2* fusion construct did not show toxicity to the cells; instead, it provided protection when challenged with H_2O_2 or hypochlorite and displayed mild sensitivity to zinc stress compared to null mutants or the wild-type strain (Figure 1C, 1D). Hypochlorite is capable of oxidatively attack numerous biological molecules as well as causing dose-dependent depletion of reduced glutathione (Kwolek-Mirek et al., 2011). The null mutants were more susceptible to hypochlorite, H_2O_2 and temperature stresses, suggesting that Dmo2p may play a role in proteostasis and cellular redox equilibrium. The levels of *DMO2* expression in different constructs were compared after adding a hemagglutinin A (HA) tag at the C-terminus of the protein. As expected, *GAL10-DMO2-HA* showed higher levels of Dmo2p-HA compared to other constructs when cells were cultured in galactose (Figure S3).

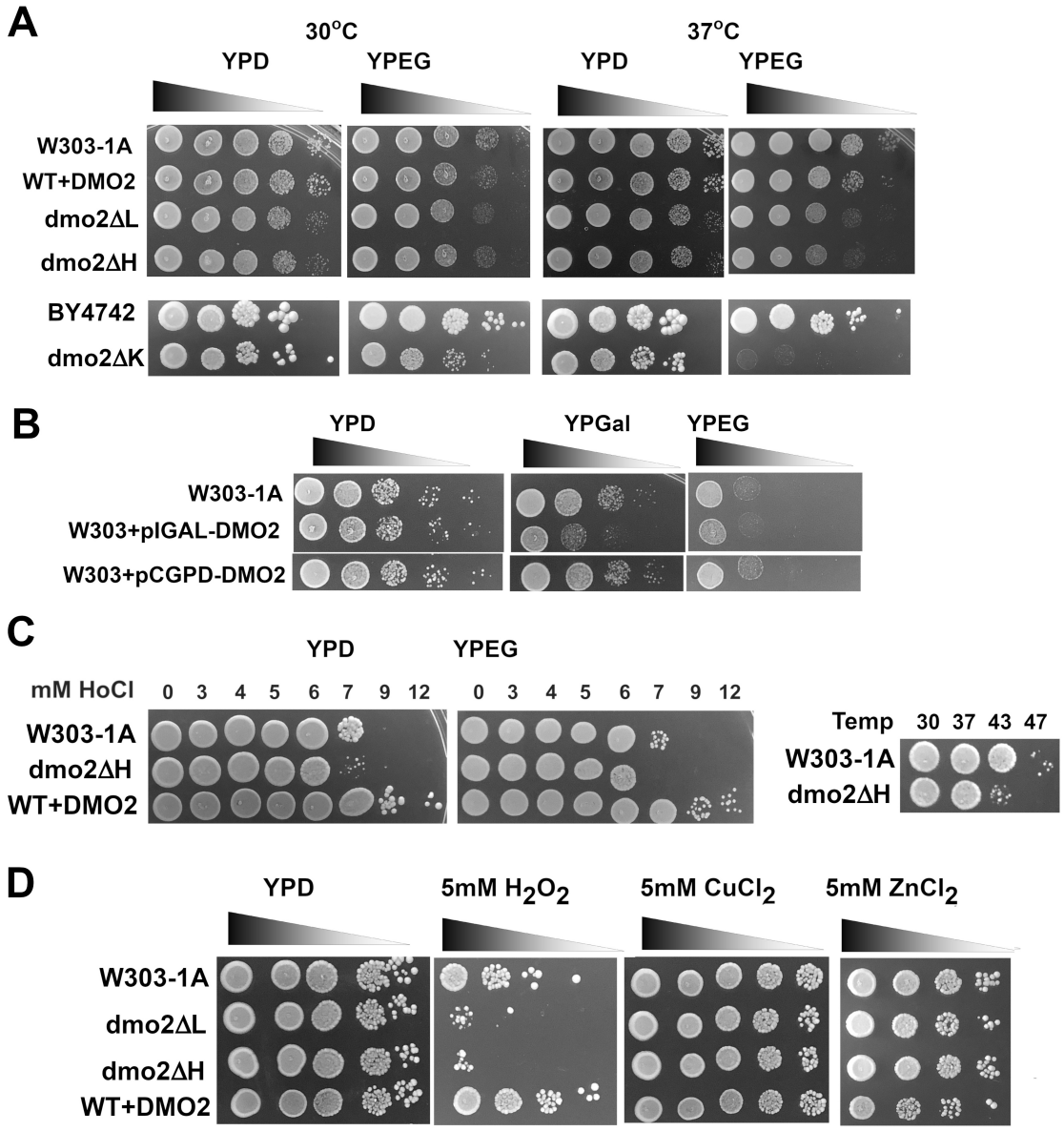

Figure 1 – Growth properties of *dmo2* mutants (A) Serial dilution test in rich fermentable glucose medium (YPD) and rich non-fermentable ethanol-glycerol medium (EG). Images related to W303 genetic background (Analyzed strains were parental W303-1A, the transformed wild-type with a *DMO2* multicopy plasmid (WT+DMO2); *DMO2* mutants *dmo2::LEU2* (dmo2ΔL) and *dmo2::HIS3* (dmo2ΔH)) were photographed after 1

day of growth, while the panels related to BY4742 genetic background, the parental strain and *dmo2::kanMX* (dmo2ΔK) mutant were obtained after 2 days of growth. **(B)** Serial dilution test in rich glucose medium (YPD), rich galactose medium (YPGAL) and rich ethanol-glycerol medium (EG) with strains W303-1A and overexpressing *DMO2* in *GAL10* promoter (W303+pIGAL-DMO2) and in *GPD* promoter (W303+pCGPD-DMO2). Plates were photographed after 1 day of growth. **(C)** Hypochlorite and temperature challenges. Cells were incubated for 5 hours in different concentrations of hypochlorite (left panel) and for 2 hours at different temperatures (right panel) before being plated in the indicated medium and grown at 30ºC for 2 days. Analyzed strains were parental W303-1A, *DMO2* mutants *dmo2::LEU2* (dmo2ΔL) and *dmo2::HIS3* (dmo2ΔH), and W303 overexpressing *DMO2* with *GPD* promoter (WT+DMO2). **(D)** Serial dilution tests in rich glucose medium (YPD) and YPD supplemented with 5mM H_2O_2, 5mM $CuCl_2$ and 5mM $ZnCl_2$ respectively. Analyzed strains were the same as in (C). The gray bar at the top of each panel represents the number of spotted cells and it will also be present in the upcoming figures depicting growth capacities.

Considering the observed growth deficit of *dmo2Δ* cells on non-fermentable carbon sources at 37ºC, and its reported deficiency in mitochondrial translation (Dickinson et al., 2022), we evaluated the mitochondrial translation and turnover of the newly synthesized products in *dmo2Δ* cells. After a 20-minute *in vivo* labeling pulse, the translated products were chased for 45 minutes. Differently of the reported data (Dickinson et al., 2022), under our experimental conditions, the labeling time can be an issue, we did not observe a significant deficit in the accumulation of mitochondrial products that could account for a general

translation deficiency. However, the mutant *dmo2Δ* exhibited higher turnover of the Cox2p product (Figure 2A). This instability of Cox2p in *dmo2Δ* cells affected its steady-state level, particularly in mitochondria isolated from cells grown at 37°C (Figure 2B). Previous proteomic data also revealed a notable reduction in the abundance of Cox2p compared to the wild-type (Figure S1). Densitometry analysis of bands for Cor1p, Cox1p, and Cox2p was performed using the histogram component of GNU Image Manipulation Program GIMP 2.10.28 with normalization to porin. The *dmo2Δ* extracts showed less than 50% of the wild-type Cox2p. Except for Cor1p and Cox1p under the 37°C condition, the other tested proteins did not show any clear decrement in their steady-state level in the *dmo2* background (Figure 2B). Accordingly, the enzymatic activity of cytochrome *c* oxidase, NADH ubiquinol cytochrome *c* reductase, and the ATP synthase activity were diminished in the mitochondria isolated from *dmo2Δ*, particularly in those grown at 37°C (Figure 3A, 3B). The impaired respiratory capacity of *dmo2Δ* at 37°C was also reflected in the formation of mitochondrial supercomplexes (Figure 3B). Moreover, considering the reported effect of human Dmo2p homolog in respiratory supercomplexes formation by modulating complex I distal arm (Stroud et al., 2016), we evaluated whether Dmo2p directly affects the formation of the yeast respiratory supercomplexes (Figure 3B), even though this yeast lacks respiratory complex I. We observed a decrease in supercomplex formation and ATP synthase dimers in the absence of Dmo2p. Previous proteomic data also indicated a reduction in Atp20p, a protein required for ATP synthase dimerization (Reinders et al., 2007), in the *dmo2* mutant (Figure S1A), which can also explain the lower content of ATP synthase dimers.

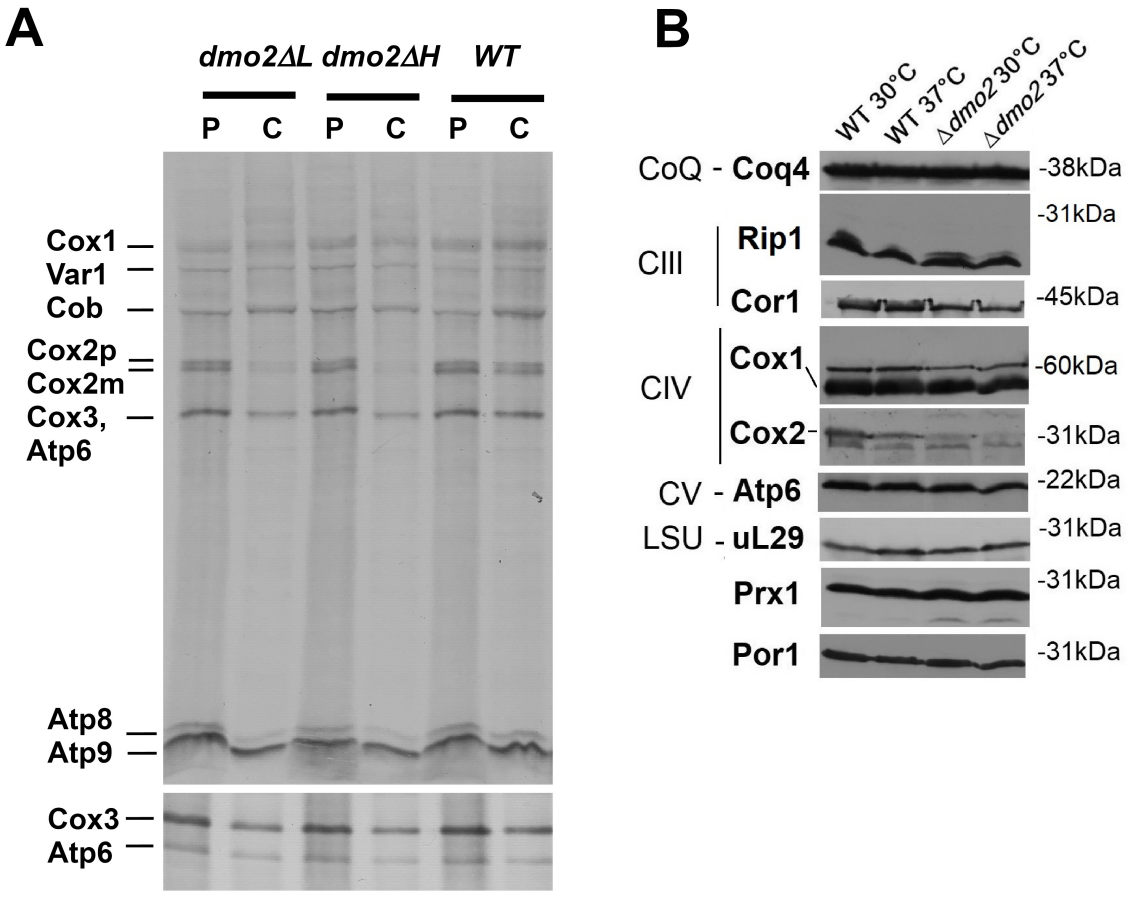

Figure 2 – Δ*dmo2* translation properties and mitochondrial proteins steady-state (A) *In vivo* labeling pulse and chase. Cells were treated with cycloheximide for 10 minutes and incubated with ^{35}S methionine/cysteine mix for 20 minutes (pulse, P). Following that, methionine/cysteine mix was added and cells were incubated for 45 minutes (chase, C). Radiolabeled mitochondrial products were separated and are indicated in the margins of the figure as follows: Cox1, Cox2 and Cox3 forming the catalytic core of cytochrome c oxidase; Atp6, Atp8 and Atp9 components of the ATP synthase; Cob, component of ubiquinol cytochrome c reductase; mitoribosome protein Var1. **(B)** Steady state protein levels of W303 (WT) and W303Δ*dmo2* (Δdmo2) mitochondria from cells grown at 30°C and 37°C. Coq4 is a component of the CoQ synthome (CoQ); Rip1 and Cor1 are

components of respiratory complex III (CIII); Cox1 and Cox2 are components of respiratory complex IV (CIV); Atp6 is a component of ATP synthase, or complex V (CV); uL29 is a component of the mitoribosome large subunit; Prx1 is a soluble mitochondrial protein and Porin is a protein from the mitochondrial outer membrane.

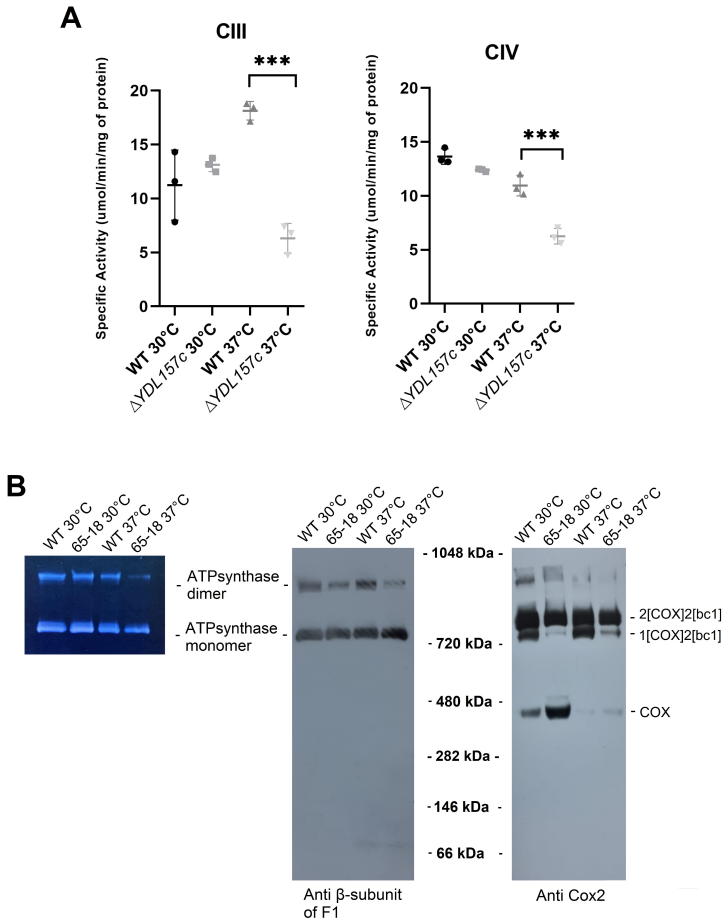

Figure 3 – Δ*dmo2* mitochondrial complexes activity assays and supercomplex formation (A) Mitochondrial respiratory complexes III (left panel) and IV (right panel) enzymatic activity assays. Complex III activity was measured by the rate of cytochrome *c* reduction, and complex IV activity was assessed by the rate of reduced cytochrome *c* oxidation. Data were obtained by three independent measures and analyzed in GraphPad

Prism (La Jolla, CA, USA) *p<0,05 *versus* WT. **(B)** WT and Δ*dmo2* mitochondria isolated from cells grown at the indicated temperatures were extracted with 2% digitonin. Extracts were loaded to a non-denaturing 4-13% acrylamide gradient BN-PAGE gel. The gel on the left illustrates ATPase in gel activity assay as described in methods. For middle and right panels, proteins separated in the gel were transferred to a PVDF membrane and probed with anti-subunit β of F1 ATP synthase (middle) and anti-hsCox2 (right).

Dmo2p intramitochondrial localization and distribution

Dmo2p has been detected in highly purified mitochondria in high-throughput studies (Reinders et al., 2006), Kyte & Doolitle hydropathy scale predicts two transmembrane domains, which can also be noticed in Dmo2p alpha-fold modeled structure (Figure S4). The Dmo2-HA tagged version enables us to follow its distribution and solubilization properties after sonication with or without carbonate, as well as its distribution in mitochondria and mitoplasts subjected to proteinase K digestion. Dmo2p is not solubilized with sodium carbonate confirming its predicted membrane association (Figure 4A), moreover, the protein is susceptible to proteinase K after the osmotic removal of the outer membrane, indicating that its C-terminus is exposed to the intermembrane space. The outer-membrane removal by hypotonic shock was confirmed by the substantial loss of the soluble intermembrane marker cytochrome b2 and supported by the decrease of Sco1p molecular weight as a result of the proteinase K digestion; therefore, Dmo2p has the same topology as the one described for Sco1p (Glerum et al. 1996b). The matrix protein α-ketoglutarate dehydrogenase (Repetto and Tzagoloff, 1990) was protected against

proteinase K in all conditions confirming the intactness of the inner membrane in the mitoplasts (Figure 4B).

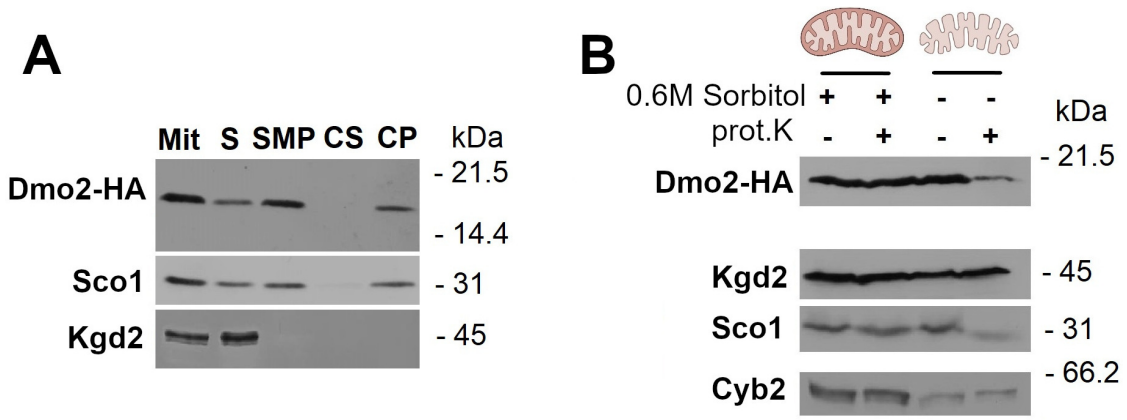

Figure 4 Dmo2p is in the mitochondrial inner membrane facing the intermembrane space. (A) Membrane solubility assay. 200µg of mitochondria isolated from W303/*DMO2*-HA construct were sonicated for 10 seconds at 80% amplitude and centrifuged at 30,000 × g for 30 minutes. Supernatant (S) and part of the pellet (SMP) were collected. Pellet was resuspended in 0,2M sodium carbonate, incubated in ice for 30 minutes and centrifuged again as before. Supernatant (CS) and pellet (CP) were collected. Fractions were separated in a 12% acrylamide SDS-PAGE gel, transferred to nitrocellulose membrane, and probed with anti-HA, anti-Sco1 and anti-Kgd2 as control for soluble proteins. Mitochondria are indicated as Mit. **(B)** Intramitochondrial localization of Dmo2. 400µg of mitochondria from W303/*DMO2*-HA strain were suspended in 0.21ml of 10mM HEPES buffer pH 7.5 with (+) or without (-) 0.6M sorbitol to create an osmotic challenge; and with (+) or without (-) Proteinase K at a final concentration of 100 µg/ml. After one hour of incubation on ice, PMSF was added at a final concentration of 0.5mM. Mitochondria and mitoplasts were centrifuged at 20K rpm (Beckman TLA-55 fixed angle rotor) for fifteen minutes. Pellets

were suspended in 10µl of 50% TCA and centrifuged again in tabletop centrifuge for five minutes. Pellets were suspended in Laemmli buffer (Laemmli, 1970). Proteins were separated in standard 12% acrylamide SDS-PAGE gel, transferred to nitrocellulose membrane and probed with anti-HA, anti-Sco1, anti-Cyb2 and anti-Kgd2.

Dmo2p distribution and putative complex formation were investigated using sucrose gradients followed by ultracentrifugation. The Dmo2-HA product fractioned in the middle of the gradient; it displayed a weight higher than the 144 kDa lactate dehydrogenase marker. This indicates that Dmo2p is part of a large high molecular complex. We then hypothesized that Dmo2p may be associated with ancillary proteins of Cox2p, such as Sco1p and Sco2p, which share the same inner membrane localization and topology as Dmo2p. Taking advantage of available antibodies (kindly provided by A. Tzagoloff) we observed co-sedimentation of Dmo2p with Sco1p and Sco2p (Figure 5). We used anti-Prx1 (gift from M. Demasi) as a sedimentation control of a mitochondrial antioxidant enzyme. Moreover, mitochondrial Prx1p is a peroxiredoxin required for hydroperoxides reduction dependent on glutathione (Pedrajas et al., 2000) and exhibits different electrophoretic mobility variants, with the lower mobility version found in the bottom of the gradient, consistent with its reported association with mitoribosomes assembly intermediates, while higher mobility versions of Prx1p sediment in lighter fractions not coincidently with Dmo2p (Kaur and Stuart, 2011; Gomes et al. 2017; Chagas et al., 2022).

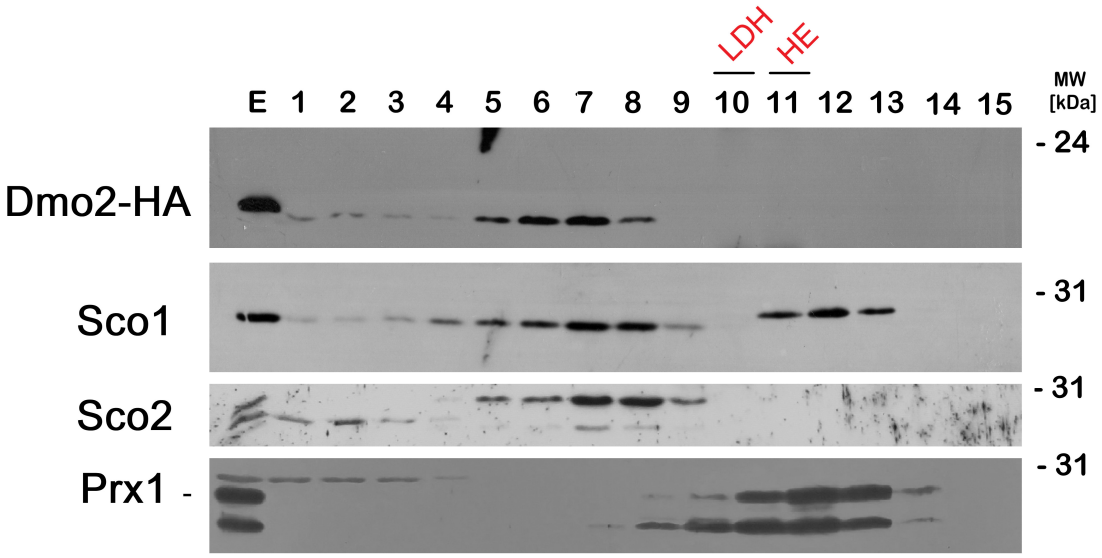

Figure 5 – Dmo2 has a sedimentation pattern similar to Sco1 and to Sco2 in a sucrose gradient. Extracts from W303/DMO2-HA were mixed with hemoglobin (64kDa) and lactate dehydrogenase (144kDa), applied on a 7-20% sucrose gradient and centrifuged as described in methods. Gradient fractions were separated in a 12% acrylamide SDS-PAGE gel. Proteins were transferred to a nitrocellulose membrane and probed with anti-HA, anti-Sco1, anti-Sco2 and anti-Prx1 as shown. Prx1 was used as control for lighter fractions.

Dmo2p is required for the stabilization of unprocessed Cox2p and physically interacts with Cox2p.

The elevated Cox2p turnover in *dmo2Δ* cells (Figure 2A) was further investigated by combining the *dmo2Δ* mutant with null mutants of Cox2p processing factors, namely *imp2*, *cox18*, *cox20*, and *sco2*. The translocation of Cox2p C-terminus transmembrane domains depends on Cox18p, and in its absence, only the N-terminus domain can cross the inner membrane while the C-terminus remains exposed in the matrix side (Fiumera et al.,

2007). Imp2p is part of the peptidase complex required for the removal of Cox2p N-terminus pre-sequence (Nunari et al., 1993). In both mutants, the newly synthesized Cox2p is clearly detected after the chase, but most of the signal is lost when the *dmo2* mutation is also present (Figure 6). Cox20p acts as a chaperone for Cox2p, protecting it from degradation and facilitating the membrane insertion of the newly synthesized product through copper metalation by Sco1p and Sco2p (Hell et al., 2000; Eliot et al., 2012; Bourens et al., 2014; Lorenzi et al., 2016; Bourens and Barrientos, 2017). As expected, in the *cox20* mutant the Cox2p product presents elevated turnover, but this effect is exacerbated when combined with the *dmo2* mutation. Finally, while the *sco2* mutant did not show any particular deficiency, the double mutant *sco2Δ dmo2Δ* not only displayed decreased the stability of Cox2p but also showed a general impairment in mitochondrial translation (Figure 6A).

The phenotypes of the *dmo2Δ* mutants in Cox2p stability, as well as the co-localization (Figure 4B) and co-sedimentation of Dmo2p with Sco1p and Sco2p (Figure 5) suggest a potential physical association between their products. To test this hypothesis, pull-down assays were performed using yeast strains containing integrated single copy genes expressing Dmo2p with its C-terminal fused to protein C epitope followed by polyhistidine (Dmo2p-CH). Mitochondrial proteins were extracted using digitonin and Dmo2p-CH was immunopurified on protein C antibody beads. Western blots of the eluate from the protein C antibody beads were probed with antibodies against the protein C epitope to detect Dmo2p-CH, as well as antibodies against Sco1p, Sco2p, Cox2p, and porin (Figure 6B). In these experiments, Sco1p, Sco2p, and Cox2p co-immunopurified with Dmo2p, whereas only a small amount of Cox2p was pulled down in a strain expressing

non-tagged native Dmo2p. The co-purification of Cox2p led to further investigation of this fraction using a native gel. Therefore, pull down elution fractions from wild type and Dmo2p-CH mitochondrial extracts were also loaded to a BN-PAGE 4-13% polyacrylamide gel and immunodecorated with anti-protein C and anti-hsCox2 (Figure 6C). As shown in this panel, *bc*1 and COX supercomplexes with conformations 2[*bc1*] 2[COX] and 2[*bc1*] 1[COX] and estimated sizes of 1000 kDa and 750 kDa respectively (Schägger and Pfeiffer, 2000) were pulled down in the Dmo2p-CH eluate, suggesting the involvement of Dmo2p in these structures, as well as its human ortholog DMAC1 gene product (Stroud et al., 2016). Anti-Cox2p also detected a clear band in the middle of the gel that probably corresponds to COX 200 kDa estimated size, but further experiments are required to determine if it represents free COX or Cox2p assembly intermediates. Additionally, anti-protein C probing unveiled a broad smear extending from the bottom to the region where the supercomplexes were detected, indicating its stable interaction with multiple mitochondrial proteins.

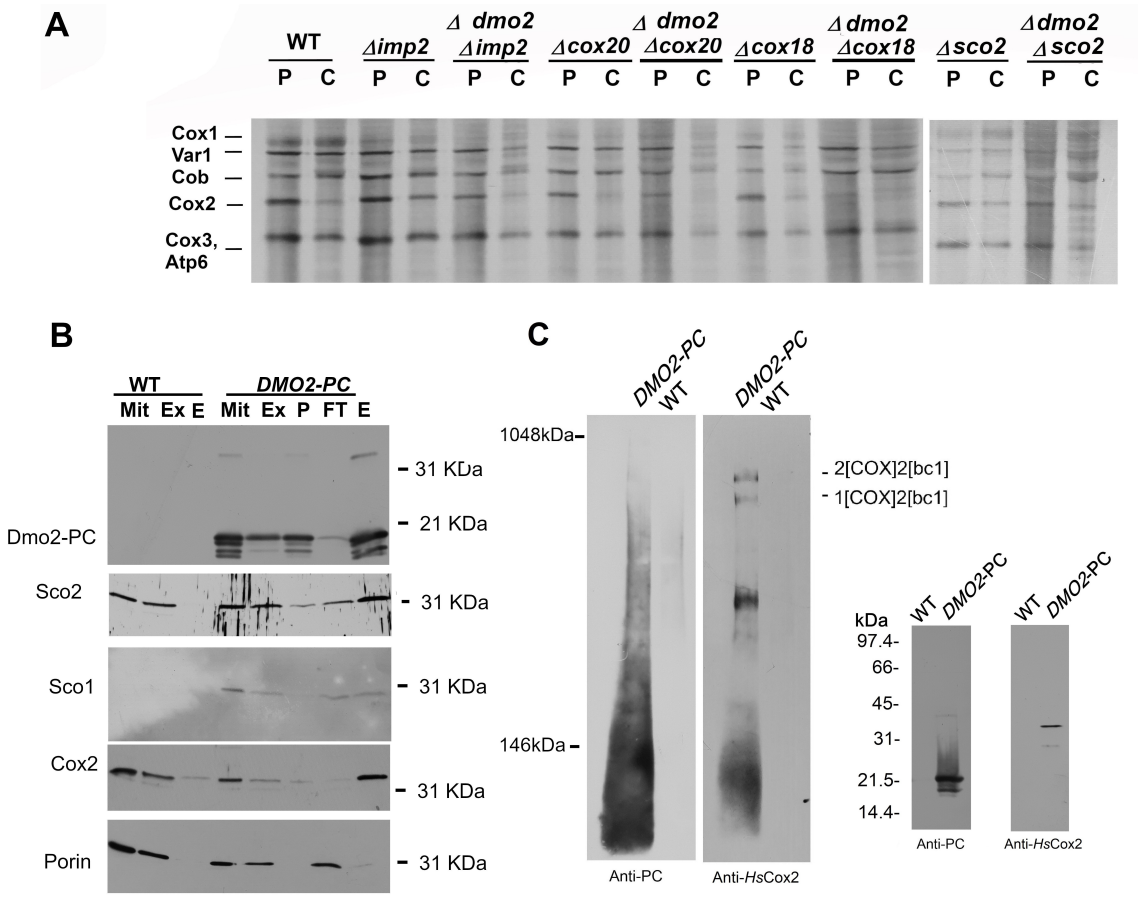

Figure 6 –Genetic and physical associations of *DMO2* with *COX2*. (A) *In vivo* labeling pulse and chase. Cells were treated with cycloheximide for 10 minutes and incubated with ^{35}S methionine/cysteine mix for 20 minutes (pulse, P). Following that, methionine/cysteine mix was added and cells were incubated for 45 minutes (chase, C). Radiolabeled mitochondrial products were separated and are indicated in the margins of the figure as in Figure 2(A). **(B)** Pull down assays. 50µg of mitochondria (Mit) from WT and W303/DMO2-PC strains were extracted with 200µl 2% digitonin generating extraction (Ex) and a pellet (P) fractions. The extracts were incubated with protein C antibody beads. Non-ligand fractions (Ft) were discarded and ligands were eluted from the beads with

EDTA (E). Elution fractions are five times more concentrated than extraction fractions. **(C)** Pull down elutions from WT and W303/DMO2-PC were loaded to a 4-13% non-denaturing BN-PAGE gel (left panel) and standard 12% acrylamide SDS-PAGE gel (right panel).. Proteins were transferred to a PVDF membrane and probed with anti-protein C and anti-hsCox2 antibodies.

DMO2 overexpression suppresses cox23Δ null mutant respiratory growth deficiency.

We hypothesized that if Dmo2p functions in the Cox2p metalochaperone complex, it may exhibit genetic interactions with genes implicated in Cox2p module assembly. To investigate this, we examined the growth of the double mutants *cox20Δ dmo2Δ* and *sco2Δ dmo2Δ* on non-fermentable carbon sources. It is known that *cox20Δ* mutants can revert to respiratory competence, albeit with a relatively high frequency, through the bypass action of *yme1*, *mgr1,* or *mgr3* mutations (Elliot et al., 2012). On the other hand, the *sco2Δ* mutant does not display growth impairments (Figure S4, Glerum et al., 1996a). We observed that the double mutant *cox20Δ dmo2Δ* retained the ability to revert to respiratory competence, although at a lower frequency compared to the single *cox20Δ* mutation (Figure S5). A possible reason for the lower reversion is the increased instability of Cox2p in the double mutant *cox20Δ dmo2Δ* (Figure 6). Additionally, we noticed that the addition of *sco2Δ* mutation slightly aggravated the growth capacity of *dmo2Δ* (Figure 7A). This negative interaction between the two mutants was initially observed in synthetic genetic array studies (Figure S2, Usaj et al., 2017). We further explored the genetic connection by transforming *dmo2Δ* with various plasmids harboring genes involved in Cox2p maturation such as *SCO1*, *SCO2*, *COX17*, *COX18*, *COX19*, *COX23*, but no improvement in growth

was observed (data not shown). However, when the respective mutants for the aforementioned genes were transformed with a multicopy plasmid harboring *DMO2* (Figure S6), we observed partial suppression of the *cox23*Δ respiratory growth deficiency (Figure 7B). Extra Dmo2p suppresses *cox23*Δ respiratory in the two parental backgrounds, and after a four-hour challenge with hypochlorite (Figure 7C). The addition of copper did not affect the suppressive growth capacity. Notably, *COX17* is also a multicopy suppressor of *cox23Δ*, but its suppression relies on the presence of extra copper in the medium (Barros et al., 2004), and the I101F point mutation in *COX1* partially alleviates the requirement for *COX23* (Dela Cruz et al., 2016). While the functions of Cox23p remain largely unknown, it is known to participate in the regulation of mitochondrial copper homeostasis and distribution (Barros et al., 2004; Longen et al., 2009; Dela Cruz et al., 2016). Dmo2p may potentially play a similar role in copper homeostasis and distribution within mitochondria.

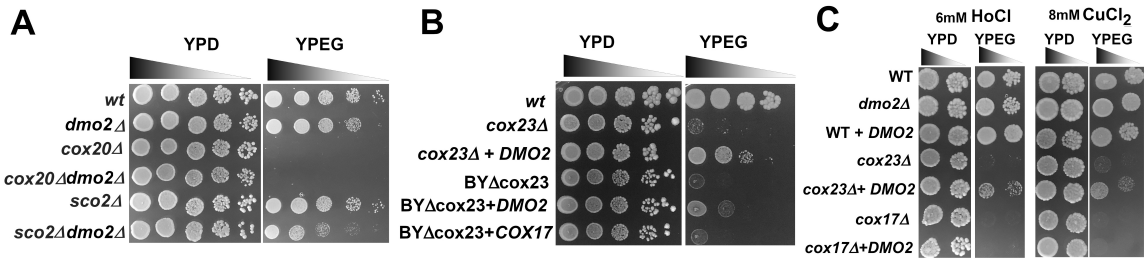

Figure 7 - Overexpression of *DMO2* partially rescues *cox23* phenotype (A) Serial dilution test in YPD and YPEG media of strains: W303-1A (wt), *dmo2*Δ, *cox20*Δ, *cox20*Δ*dmo2*Δ, *sco2*Δ and *sco2*Δ*dmo2*Δ. Plates were incubated at 30°C or 37°C as indicated and photographed after two days of growth. **(B)** Serial dilution test in YPD and YPEG media of strains W303-1A (wt), *cox23*Δ and *cox23*Δ harboring a YEp351-*DMO2* with *DMO2*'s endogenous promoter plasmid (*cox23*Δ + *DMO2*). Growth of the *cox23Δ* mutant in the BY4742 background (BYΔcox23) were also compared to the transformed mutant with *DMO2* (BYΔcox23) and *COX17* (BYΔcox23). **(C)** Serial dilution tests in YPD and YPEG media of the strains indicated in the figure with W303 genetic background. Cells were challenged for four hours in rich glucose media supplemented with 6mM hypochlorite (left panel) and 8mM copper chloride (right panel) before being plated onto YPD and YPEG plates. Images were obtained after 2 days of growth.

Evaluation of Dmo2p requirement for stresses responses and redox control

As discussed in previous sections, *dmo2Δ* mutants exhibit growth defects at high temperatures, altered sensitivity to stressors, and instability of newly synthesized Cox2p. To investigate the potential role of Dmo2p in cell proteostasis, we examined whether *dmo2Δ* cells could adapt to heat shock responses as demonstrated in Susan Lindquist's classic experiment (Yost and Lindquist, 1991). Wild-type cells and *dmo2Δ* mutants were

incubated at 37°C for 15 minutes, while another set of the same strains was kept at 23°C. As expected, wild-type cells exhibited greater resistance to subsequent heat shock treatments, whereas the *dmo2Δ* mutant did not (Figure S7).

Another piece of evidence that links Dmo2p to redox control and proteostasis lies in the presence of two conserved cysteines present in the N-terminus (Figure S4). Cysteine residues play crucial roles in the folding, stability, and activity of numerous proteins, including chaperones, and are also involved in redox reactions, which can impact the function and regulation of chaperones (Fra et al., 2017). To explore the significance of the cysteines, we substituted C24 and C27 with serines to generate the mutants C24S and C27S. We also generated mutants with both cysteines mutated in a single allele. The *dmo2* cysteine mutants showed the same growth properties as the null mutant on ethanol-glycerol (Figure 8A), and showed increased susceptibility to oxidative stress induced by hypochlorite and hydrogen peroxide (Figure 8B). Additionally, the tagged products Dmo2-C24S-HA, Dmo2-C27S-HA, and Dmo2-C24S/C27S-HA displayed reduced stability compared to the original Dmo2-HA (Figure 8C).

Given that hypochlorite toxicity has been associated with reduced glutathione levels (Kwolek-Mirek et al., 2011), and we observed that an excess of Dmo2p resulted in increased resistance to this oxychloro compound (Figure 1C) while also impairing the respiratory growth of the null mutant, we proceeded to evaluate the redox state of the d*mo2Δ* mutant by measuring mitochondrial matrix glutathione (GSH) levels. Glutathione plays a crucial role in yeast by reducing disulfide bonds and protecting cysteines from overoxidation (Grant et al., 1996). Using a redox-sensitive GFP probe (ro-GFP) (Hanson et

al., 2004), we observed a higher content of oxidized glutathione (GSSG) in the mitochondrial matrix of the *dmo2Δ* mutant compared to wild-type cells under the same oxidant conditions (Figure 8C). This indicates a severe deficit in GSSG reduction by glutathione reductases, peroxiredoxins, thioredoxins, and glutaredoxins present in the matrix, particularly Prx1p (Calabrese et al., 2019). The imbalanced presence of GSSG in the *dmo2Δ* mutant matrix aligns with our findings from the oxidant challenges and the viability of *dmo2Δ* cells.

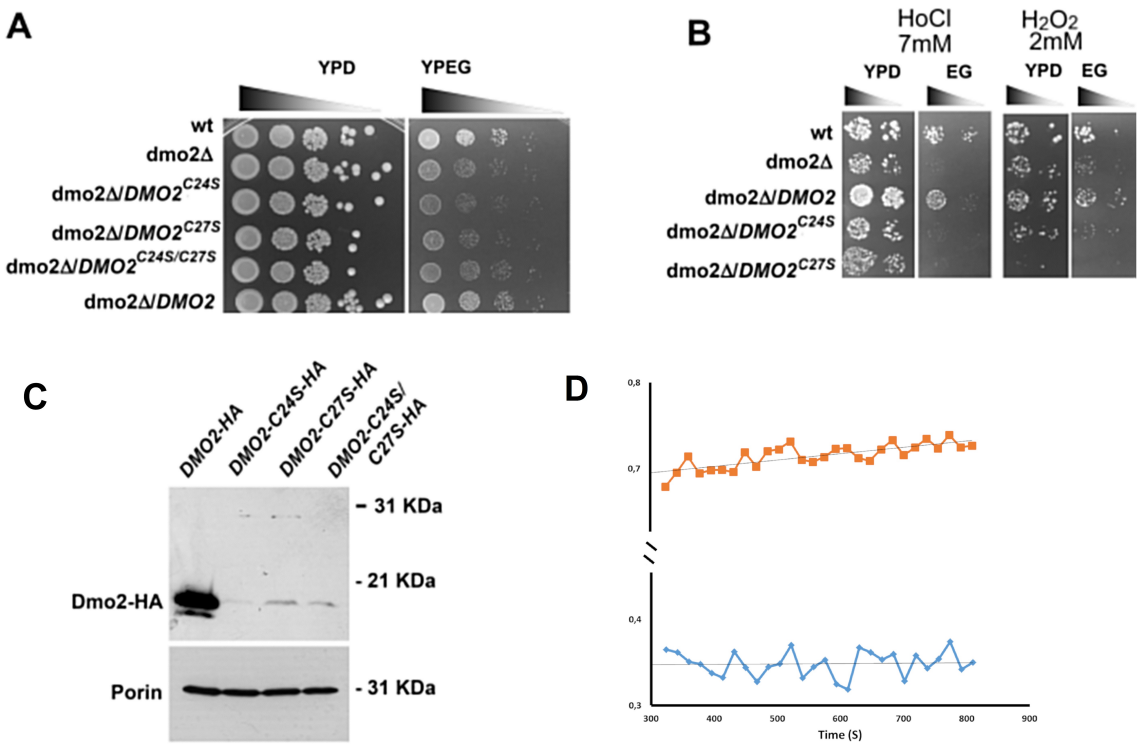

Figure 8 – Dmo2p is important for stress response and redox balance (A) Serial dilution test in rich glucose YPD and rich ethanol-glycerol non-fermenting YPEG media with strains: W303-1A (wt), *dmo2Δ* null mutant (*dmo2Δ*), *dmo2Δ* harboring a point mutation in cysteine residue 24 changing it to a serine (*dmo2Δ/DMO2*^{C24S}), *dmo2Δ* with a point mutation in cysteine residue 27 changing it to a serine (*dmo2Δ/DMO2*^{C27S}), *dmo2Δ* with both point mutations C24S and C27S (*dmo2Δ/DMO2*$^{C24S/C27S}$) and *dmo2Δ* harboring a functional copy of DMO2 with its endogenous promoter (*dmo2Δ/DMO2*). Plates were incubated at 30°C and 37°C for 1 day and photographed. **(B)** The strains described in (A) were challenged for four hours in YPD liquid media with 7mM hypochlorite (HoCl) or 2mM H2O2, and then spoted on YPD and YPEG. Plates were photographed after two days. **(C)** Proteins from mitochondria isolated from strains *DMO2-HA*, *DMO2*$^{C24S-HA}$, *DMO2*$^{C27S-}$

^{HA} and *DMO2*$^{C24S/C27S\text{-}HA}$ were separated in a standard 12% acrylamide SDS-PAGE gel. Proteins were transferred to a nitrocellulose membrane and probed with anti-HA antibody. Porin was used as loading control. **(D)** Measurement of mitochondrial matrix glutathione oxidation state was performed as described in methods. Values shown in orange correspond to *dmo2Δ* null mutant, while values shown in blue correspond to control W303-1B strain.

We conducted additional experiments to evaluate the growth capacity of *dmo2Δ* mutants on oleate, an oxidative medium known to induce peroxisome biogenesis, enhance peroxisome activity and the accumulation of peroxisome proteins (Venhuis et al., 1987). This experiment was motivated by previous findings that suggested the presence of Dmo2p outside of mitochondria, specifically associated with peroxisome membranes. A Dmo2-GFP construct was observed at the peroxisomal membrane or membrane periphery (Yifrach et al., 2022). When grown on non-fermentable oleate medium, the *dmo2Δ* null mutant exhibited no growth, while strains carrying C24S and C27S mutations showed poor growth (Figure 9A).

To investigate whether the steady-state level of Dmo2p was altered in the peroxisome-favored medium, we fractionated by differential centrifugation cultures of cells carrying the *DMO2-HA* allele. The steady-state level of Dmo2-HA was compared in organelle fractions obtained from cells grown in galactose, which favored mitochondrial biogenesis, and oleate. In both conditions, the Dmo2-HA product, migrating below the 21.5 kDa marker, exhibited similar detection properties as the other tested mitochondrial proteins Cox2p, porin, and Sco1p, while the peroxisome marker Fox3p was only detected in the extracts obtained from oleate grown cells. However, a significant amount of Dmo2-HA product was detected close to the 31 kDa marker in the organelle extract obtained from oleate-grown

cells. Dmo2-HA bands with lower mobility were also detected in our previous blots (Figure 9B), albeit not with such intensity. Interestingly, anti-Prx1p also unveiled the appearance of an additional product with lower electrophoretic mobility in the protein extracted from oleate-grown cells. Similarly, anti-Sco1p also seemed to detect additional bands with higher molecular weight in the oleate extracts. To test whether the aberrant migration bands observed for Dmo2p, Prx1p and Sco1p were due to disulfides bonds formation in the oxidative oleate medium, we treated the protein samples with DTT and heated them at 80°C and 100°C. The reducing agent treatments did not change the profiles of the anti-Sco1p bands, but they led to the disappearance of the high molecular weight bands of Prx1p and Dmo2p (Figure 9C). This indicates that the vanished bands had resulted from disulfides bonds cross-links. Since they were mainly detected in the oleate medium extracts, these bands variants are likely products of Prx1p and Dmo2p functions as antioxidant enzymes.

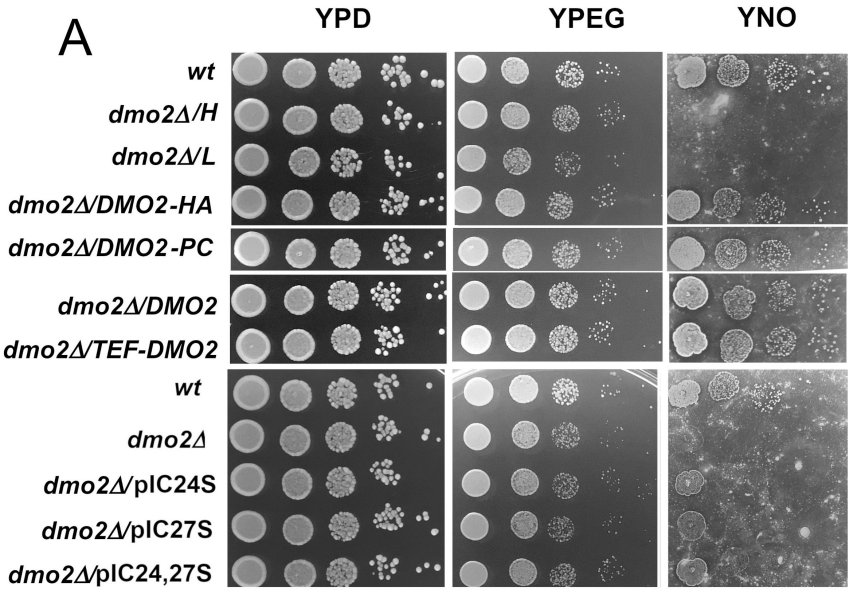
A
YPD
YPEG
YNO
wt
dmo2Δ/H
dmo2Δ/L
dmo2Δ/DMO2-HA
dmo2Δ/DMO2-PC
dmo2Δ/DMO2
dmo2Δ/TEF-DMO2
wt
dmo2Δ
dmo2Δ/pIC24S
dmo2Δ/pIC27S
dmo2Δ/pIC24,27S

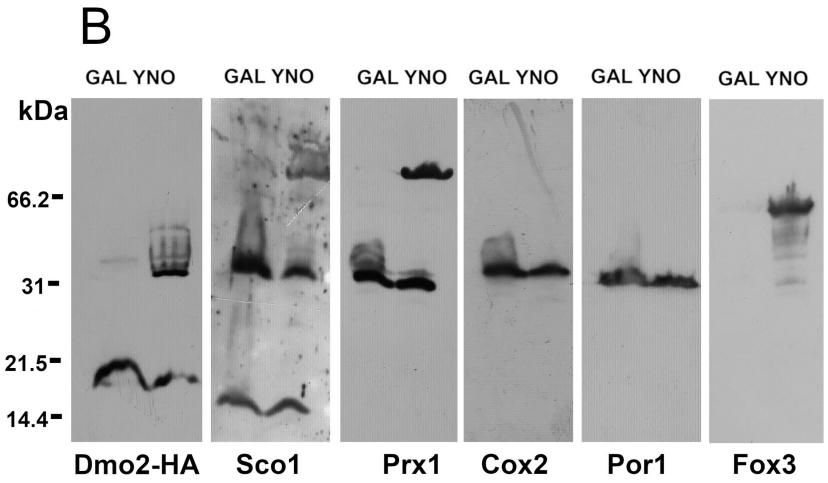
B
GAL YNO
GAL YNO
GAL YNO
GAL YNO
GAL YNO
GAL YNO
kDa
66.2
31
21.5
14.4
Dmo2-HA
Sco1
Prx1
Cox2
Por1
Fox3

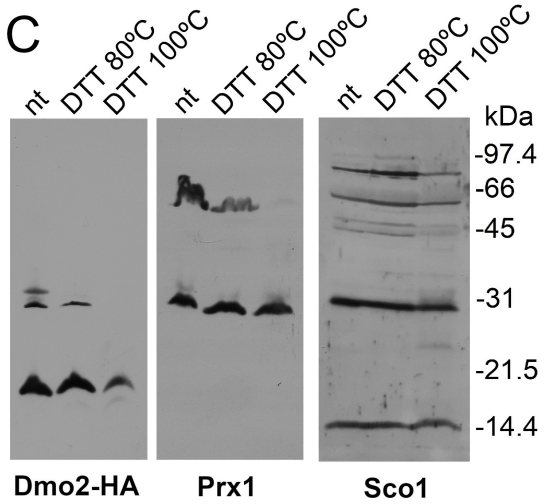
C
nt
DTT 80°C
DTT 100°C
nt
DTT 80°C
DTT 100°C
nt
DTT 80°C
DTT 100°C
kDa
-97.4
-66
-45
-31
-21.5
-14.4
Dmo2-HA
Prx1
Sco1

Figure 9 - Dmo2p may play a role in peroxisome (A) Serial dilution tests in YPD, YPEG and YNO media. Upper panel compares strains W303-1B (wt), *dmo2*Δ null mutant (*dmo2*Δ) and *dmo2*Δ harboring *DMO2* regulated by its endogenous or *TEF* promoters (*dmo2*Δ/*DMO2* and *dmo2*Δ/*TEF-DMO2* respectively). Middle panel compares W303-1B (wt), *dmo2*::*HIS3* null mutant (*dmo2*Δ*H*), *dmo2*::*LEU2* null mutant (*dmo2*Δ*L*) and *dmo2*Δ harboring *DMO2* fused with HA and Protein C (*dmo2*Δ/*DMO2-HA* and *dmo2*Δ/*DMO2-PC* respectively). Lower panel compares W303-1B (wt), *dmo2*Δ null mutant and *dmo2*Δ with cysteine to serine point mutations integrated in the mutant genome. **(B)** Mitochondria from W303/DMO2-HA were isolated after cells were grown in YPGal (GAL) and YNO to stimulate peroxisome biogenesis. Proteins were separated in a 12% acrylamide SDS-PAGE gel, transferred to nitrocellulose membrane and probed with antibodies as indicated on the bottom panel. **(C)** Protein samples from YNO grown cells were treated with 100mM DTT and heat for 5 minutes at 80°C or 100°C. The untreated extract (nt) was compared with the two treatments after probing with anti-HA (Dmo2p-HA), anti-Prx1p and anti-Sco1p.

Discussion

Dmo2p is likely involved in the mitochondrial redox metabolism; the protein is required in cells subjected to oxidative stresses as well as to heat stress, and has elevated levels of oxidized glutathione in the mitochondrial matrix. Cox2p copper metalation is a redox process that requires accessory proteins; some of them with their specific function in the process still concealed (Aich et al., 2018; Jett and Leary, 2018). It is not a surprise the need for additional proteins to accompany Cox2p and Cox1p because of the high reactivity of their intermediates that have to be chaperoned to avoid the uncontrolled generation of

reactive oxygen species (Veniamin et al., 2011; Khalimonchuk et al., 2012; Geldon et al., 2021) and the need to coordinate the assembly of these highly reactive two COX metal centers by CX_9C proteins, including *COX17*, *COX19*, *COX23*, *PET191*, and *COA6* (Longen et al., 2009; Nývltová et al., 2022). Extra copies of *DMO2* are sufficient to suppress the requirement for Cox23p. This fact strengthens the hypothesis that Dmo2p is involved in Cox2p metalation. Moreover, Dmo2p physically interacts with copper delivery enzymes Sco1p and Sco2p, as well as with Cox2p itself.

The CX_2C sequence present in *DMO2* homologs is relevant for the Dmo2p function and its steady-state level as reported here. Nevertheless, it is also possible that the removal of Dmo2p cysteines C24 or C27 impacts the import of the protein through the intermembrane space by the Mia40p relay system (Peleh et al., 2016). After cellular fractionation, we observed Dmo2p-HA present in the organelle fraction with two different sizes, one smaller than the 21.5 kDa marker, which roughly corresponds to the expected size of the tagged protein (13.5 kDa) and one product close to 31 kDa that suggestively indicate the formation of a dimer. The higher molecular weight product was majorly detected in organelle extracts obtained from stressed cells grown on oleate, suggesting that Dmo2p is a redox-regulated protein with reversible disulfide bond formation on oxidation-prone cysteine residues. Suggestively, the same was observed for the mitochondrial peroxiredoxin Prx1p. The human homolog, DMAC1 (TMEM261) contains the Cx_2C motif and it is involved in complex I distal arm assembly, supercomplexes formation (Stroud et al., 2016), and genetically connected to other genes functioning in the TCA cycle and in the OXPHOS system (Horlbeck et al., 2018). Coincidently, the *dmo2Δ* mutant also displayed a lower accumulation of respiratory supercomplexes, while the tagged protein pulled down Cox2p

and the supercomplexes. DMAC1 seems as multifunctional as its yeast homolog, and we hypothesized that it is a new example of moonlight protein. Yeast moonlight proteins have also been found to be involved in stress responses including heat shock response (HSPs) and thioredoxin peroxidase Tsa1p (Jeffery et al., 2018; West et al., 2018); the dual localization of Dmo2p strengthens this hypothesis. Dmo2p is present in the mitochondrial inner membrane, with its C-terminus exposed to the intermembrane space, a complex environment with many redox reactions (Mesecke et al., 2005). The protein is also present in the peroxisome membranes and in association with them (Yifrach et al., 2022). In yeast, peroxisomes carry out the β-oxidation of fatty acids, to generate acetyl-CoA; during this process, reactive oxygen species (ROS) are generated as byproducts. Mitochondria and peroxisome play key concert roles in the metabolism of ROS; with related evolutionary origin (Bolte et al., 2015), both can proliferate by fission sharing components of the machinery (Fransen et al., 2017). Interestingly, in a peroxisome oxidative prone medium, Dmo2p and Prx1p displayed variants with lower eletrophoretical mobility, which are removed after treatment with heat and a reducing agent.

Altogether, our data suggest a broad function of Dmo2p in redox mediated processes with impact in different oxidative processes. Similar situations have also been described for other mitochondrial proteins with a multitude of functions. Cox20p, for instance, participates in various steps of Cox2p maturation (Elliot et al., 2012) and its expression was associated with reduced levels of ROS in hydrogen peroxide and metal-induced stress (Keerthiraju et al., 2019). The present study opens up a plethora of possible investigations to ascertain the redox dynamics and partners of Dmo2p, which can also be relevant for DMAC1 and its impacts on human health.

Material and Methods

Yeast strains and growth media

The genotypes and sources of yeast strains used in this study are listed in Table 1. Yeast strains were maintained in YPD (1% yeast extract, 2% peptone, 2% glucose), YPGal (1% yeast extract, 2% peptone, 2% galactose), YPEG (1% yeast extract, 2% peptone, 2% glycerol, 2% ethanol), minimal glucose (2% glucose, 0.67% yeast nitrogen base (YNB) without amino acids, supplemented with auxotrophic requirements), YNO (0.1% oleic acid, 0.1% Tween 20, 0.67% complete YNB, 0.5% yeast extract), and sporulation media (0.5% yeast extract, 1% peptone, 0.05% glucose). All reagents, unless otherwise indicated, were obtained from Sigma-Aldrich (Saint Louis, MO).

Construction of DMO2 alleles

The *DMO2* wild-type allele was amplified from nuclear DNA with primers DMO2-F0 (5' GGCCTGCAGACTCACCCCTTAGCCT) and DMO2-2 (GGCGGATCCATTGAATGCATGCGATAAC); the 1110 bp PCR product was doubled digested with BamH1 and Pst1 and cloned in pUC18, YIp352, YEp351 (Hill et al., 1986), all previously cut with the same enzymes yielding pUC18/DMO2, pDMO2/ST1 and DMO2/ST2. The pUC18/DMO2 was used as a template for a new PCR cycle with the bi-directional primers GGCAGATCTTGTTTTTCACCACTTGCT and GGCGGATCCATTGAATGCATGCGATAAC resulting in a clean deletion of *DMO2*. The linear product containing *DMO2* flanking region in pUC18 was digested with Bgl2 and ligated to *HIS3* and *LEU2* on an approximately a 1.2 kb BamH1 fragment of DNA. The *dmo2::HIS3* and *dmo2::LEU2* null allele were recovered from the recombinant plasmids as

a 1.5 kb Pst1-BamH1 fragment and were substituted by one-step gene replacement for the wild type allele in the yeast strain W303-1A.

DMO2 C-terminal was fused to the HA tag by PCR amplification with DMO2-F0 and5'GGCATGCATTCAAGCGTAGTCTGGGACGTCGTATGGGTAGTTAGCCTGTG TTTCACCATC (DMO2-HA) primers. This PCR product contains the *DMO2* endogenous promoter, and it was cloned into YIp352 and afterwards transferred to YIp349 (Hill et al., 1986). A second PCR amplification using DMO2-HA and 5' GGCGGATCCATGAGTAATATTTTGGCAGT primers amplified only the *DMO2* coding sequence. This PCR product was cloned into YIp351-TEF1, YIp351-GPD, and YIp351-GAL (Zampol et al., 2010) in which the coding sequence of *DMO2-HA* allele is under control of the *GAL10* promoter, the translation elongation factor 1α promoter (*TEF1*) and the glyceraldehyde-3-phosphate dehydrogenase promoter (*GPD*) (Mumberg et al., 1995). The DMO2-PC fusion was obtained using primers DMO2-F0 and 5' GGCCTGCAGGTTAGCCTGTGTTTCACCATC primers, digested with Pst1 and cloned in frame with the protein C sequence present in YIp351-CH plasmid.

The cysteine point mutants were created by site-directed mutagenesis using two PCR reactions. In each reaction one primer annealed to the desired region and creates the mutation and an Nco1 site. For reaction 1 the following pair de primers were combined to generate the indicate mutation: $dmo2^{C24S}$ DMO2-2 with 5' GGCCCATGGATTCCGTTCCTTGTCAAGTC; $dmo2^{C27S}$ DMO2-2 with 5' GGCCCATGGATTGCGTTCCTTCTCAAGTC; $dmo2^{C24S,C27S}$, DMO2-2 with 5' GGCCCATGGATTCCGTTCCTTCTCAAGTC. The second reaction were the same for the three mutants and used the pair DMO2-F0 with

5´GGCCCATGGTCTCTTCTTTTTCCAGCTCC. The products of reaction 1 were digested with Nco1 and BamH1, and products of reaction 2 digested with Nco1 and Pst1. The double digested fragments were cloned into YIp352, YIp349 and YEp351 (Hill et al., 1986)

Mitochondrial Protein Synthesis

Yeast cells cultures were cultured in rich galactose media. Mitochondrial translation products were labeled in whole cells with a mixture of [^{35}S] methionine and [^{35}S] cysteine (7 mCi/mmol) in the presence of cycloheximide. Cells were lysed and protein extracted as previously described (Santos et al., 2021). Total cellular proteins were separated by SDS-PAGE on 17.5% polyacrylamide or 6M UREA-PAGE on 12.5% polyacrylamide gel systems.

Antibodies

We acknowledge the donation of the antibodies used in this work: A. Tzagoloff – Columbia University (Anti-Rip1, Anti-β subunit of F1, Anti-Cox1, Anti-Cox2, Anti-Cytb2, Anti-Kgd2, Anti-Sco1, Anti-Sco2) ; JP D-iRago – Univ. Bordeaux (Anti-Atp6); C. Clark – UCLA (Anti-Coq4) W. Girzalsky - Ruhr University (Anti-Fox3); M. Demasi – I.Butantã (Anti-Prx1); Martin Ott - Stockholm University (Anti-uL29). Anti-porin was bought from Thermofisher (Waltham, MA - USA) and anti-hsCox2 from Abcam (Cambridge, MA – USA). .

Mitochondria isolation and fractionation

Yeast mitochondria were prepared by the method of Herrmann et al. (1994) using Zymolyase 20T – Zymo-Research (Irvine, CA) to obtain spheroplasts. Protein

concentrations were determined by the method of Lowry et al (1951). Six mg of mitochondrial preparation were solubilized in 400 µL of an extraction buffer (20 mM Hepes pH 7.4, 25 mM KCl, 0.5 mM PMSF, 0.8% Triton X100 (or 2% Digitonin), 5 mM $MgCl_2$) and were centrifuged at 27,000 × g for 15 minutes and layered onto a 7 to 20% linear sucrose gradient containing 10 mM Tris-Cl pH 7.5, 0.5 mM EDTA and 0.05% Triton X-100. The gradient was centrifuged at 54,000 rpm for 5 hours in a Beckmann SW55Ti rotor. The gradient was collected by gravity in 16 equal fractions and each fraction was assayed for hemoglobin by absorption at 410 nm and for lactate dehydrogenase by measuring NADH-dependent conversion of pyruvate to lactate.

Enzymatic assays of mitochondrial respiratory complexes

Ubiquinol-cytochrome *c* reductase activity was measured by following the increase in absorbance at 550 nm due to the reduction of cytochrome *c* in the presence of 10mM NADH (NCCR). COX was assayed by following the oxidation of ferro-cytochrome at 550nM (Tzagoloff et al., 1975). ATPsynthase in gel assays were performed as described elsewhere (Franco et al., 2019). 50µg of mitochondria were extracted with 2% digitonin and loaded to a 4–13% non-denaturing blue native gel (BN-PAGE).

Mitochondrial matrix gluthatione oxidation state meaurements

W303-1B and *dmo2Δ* mutants were transformed with the plasmid p416-Su9-Grx1, which addresses to the mitochondrial matrix the modified ro-GFP (Morgan et al., 2011). We follow a protocol described elsewhere (Calabrese et al., 2019). The transformants were grown in galactose minimal media without uracil for plasmid selection at 30°C. The cells

were harvested by centrifugation at 1,500 × g for 3 minutes at room temperature and subsequently suspended in 0.1 M sorbitol, 0.1 M Tris-HCl pH 7.4, 0.1 M NaCl to a final concentration of 1.5 OD600 units/ml; 180 µl of cells were transferred to appropriate microplates. To one well, diamide was added as the fully oxidized control. To a second, DTT was added as the fully reduced. Fluorescence was recorded using filter optics at excitation wavelengths of 410 ± 5 nm and 482 ± 8 nm, and an emission wavelength of 530 ± 20 nm. A basal response was measured for 10 minutes, then the sample cell wells were challenged with H_2O_2 1mM and the response was followed for 60 minutes.

Miscellaneous procedures

Protein concentrations were determined by the method of Lowry (Lowry et al., 1951), and were suspended with the Laemmli buffer (Laemmli, 1970) for SDS-PAGE blot analyses. For BN-PAGE, mitochondrial proteins were extracted with 2% final concentration of digitonin and separated on a 4-13% linear polyacrylamide gel under non-denaturing conditions, proteins were transferred to a PVDF membrane and probed with antibodies indicated in the Figures (Franco et al., 2019). The antibody-antigen complexes were visualized with coumaric acid, luminol and hydrogen peroxide mixture. Densitometry analysis of the bands was done using the histogram component of GNU Image Manipulation Program GIMP 2.10.28. GraphPad Prism software was used for graphs and data analyses by one-way multiple comparisons Turkey's statistical test.

Acknowledgments

We would like to acknowledge Professor Luis Netto (IB-USP) for providing reagents and granting us access to the fluorescence reader equipment. This work was supported by grants and fellowships from Fundação de Amparo a Pesquisa de São Paulo (FAPESP 2020/05812-7, 2013/07937-8), Conselho Nacional de Desenvolvimento Científico e Tecnológico (CNPq 305054/2022-8) and Coordenação de Aperfeiçoamento de Pessoal de Nível Superior - Brasil (CAPES) - Finance Code 001. Maria Kfouri, Jhulia Chagas, Fernando Gomes, and Leticia Franco are fellowship recipients from FAPESP (FAPESP- 2022/02744-6, 2022/08559-6, 2023/01812-0, 2019/02799-2).

Author Contributions

MAKMS – Performed the experiments, analyzed the data, and prepared the digital images.

LVRF - Conceived and designed experiments.

JACH - Performed the experiments.

FG - Performed the experiments, analyzed the data.

MHB – Conceived, designed and performed experiments; prepared the digital images and drafted the manuscript.

Conflict of Interest

The authors declare that there is no conflict of interest regarding the publication of this article.

References

Aich A, Wang C, Chowdhury A, Ronsör C, Pacheu-Grau D, Richter-Dennerlein R, Dennerlein S, Rehling P. COX16 promotes COX2 metallation and assembly during respiratory complex IV biogenesis. Elife. 2018 Jan 30;7:e32572. doi: 10.7554/eLife.32572. PMID: 29381136; PMCID: PMC5809144.

Banci L, Bertini I, Ciofi-Baffoni S, Hadjiloi T, Martinelli M, Palumaa P. Mitochondrial copper(I) transfer from Cox17 to Sco1 is coupled to electron transfer. Proc Natl Acad Sci U S A. 2008 May 13;105(19):6803-8. doi: 10.1073/pnas.0800019105. Epub 2008 May 5. PMID: 18458339; PMCID: PMC2383975.

Barros MH, Johnson A, Tzagoloff A. COX23, a homologue of COX17, is required for cytochrome oxidase assembly. J Biol Chem. 2004 Jul 23;279(30):31943-7. doi: 10.1074/jbc.M405014200. Epub 2004 May 15. PMID: 15145942.

Barros MH, McStay GP. Modular biogenesis of mitochondrial respiratory complexes. Mitochondrion. 2020 Jan;50:94-114. doi: 10.1016/j.mito.2019.10.008. Epub 2019 Oct 25. PMID: 31669617.

Barros MH, Nobrega FG, Tzagoloff A. Mitochondrial ferredoxin is required for heme A synthesis in Saccharomyces cerevisiae. J Biol Chem. 2002 Mar 22;277(12):9997-10002. doi: 10.1074/jbc.M112025200. Epub 2002 Jan 11. PMID: 11788607.

Bolte K, Rensing SA, Maier UG. The evolution of eukaryotic cells from the perspective of peroxisomes: phylogenetic analyses of peroxisomal beta-oxidation enzymes support mitochondria-first models of eukaryotic cell evolution. Bioessays. 2015 Feb;37(2):195-203. doi: 10.1002/bies.201400151. Epub 2014 Nov 13. PMID: 25394329.

Bourens M, Barrientos A. Human mitochondrial cytochrome c oxidase assembly factor COX18 acts transiently as a membrane insertase within the subunit 2 maturation module. J

Biol Chem. 2017 May 12;292(19):7774-7783. doi: 10.1074/jbc.M117.778514. Epub 2017 Mar 22. PMID: 28330871; PMCID: PMC5427259.

Bourens M, Boulet A, Leary SC, Barrientos A. Human COX20 cooperates with SCO1 and SCO2 to mature COX2 and promote the assembly of cytochrome c oxidase. Hum Mol Genet. 2014 Jun 1;23(11):2901-13. doi: 10.1093/hmg/ddu003. Epub 2014 Jan 8. PMID: 24403053; PMCID: PMC4014192.

Broadley SA, Demlow CM, Fox TD. Peripheral mitochondrial inner membrane protein, Mss2p, required for export of the mitochondrially coded Cox2p C tail in Saccharomyces cerevisiae. Mol Cell Biol. 2001 Nov;21(22):7663-72. doi: 10.1128/MCB.21.22.7663-7672.2001. PMID: 11604502; PMCID: PMC99937.

Calabrese G, Peker E, Amponsah PS, Hoehne MN, Riemer T, Mai M, Bienert GP, Deponte M, Morgan B, Riemer J. Hyperoxidation of mitochondrial peroxiredoxin limits H2 O2 -induced cell death in yeast. EMBO J. 2019 Sep 16;38(18):e101552. doi: 10.15252/embj.2019101552. Epub 2019 Aug 7. PMID: 31389622; PMCID: PMC6745495.

Cerqua C, Morbidoni V, Desbats MA, Doimo M, Frasson C, Sacconi S, Baldoin MC, Sartori G, Basso G, Salviati L, Trevisson E. COX16 is required for assembly of cytochrome c oxidase in human cells and is involved in copper delivery to COX2. Biochim Biophys Acta Bioenerg. 2018 Apr;1859(4):244-252. doi: 10.1016/j.bbabio.2018.01.004. Epub 2018 Feb 3. PMID: 29355485.

Chagas JAC, Kfouri Martins Soares MA, Ribeiro Franco LV, Barros MH. Overexpression of MRX9 impairs processing of RNAs encoding mitochondrial oxidative phosphorylation factors COB and COX1 in yeast. J Biol Chem. 2022 Aug;298(8):102214. doi: 10.1016/j.jbc.2022.102214. Epub 2022 Jun 30. PMID: 35779633; PMCID: PMC9307953.

Chinenov YV. Cytochrome c oxidase assembly factors with a thioredoxin fold are conserved among prokaryotes and eukaryotes. J Mol Med (Berl). 2000;78(5):239-42. doi: 10.1007/s001090000110. Erratum in: J Mol Med 2000;78(5):243-4. PMID: 10954195.

Cobine PA, Pierrel F, Bestwick ML, Winge DR. Mitochondrial matrix copper complex used in metallation of cytochrome oxidase and superoxide dismutase. J Biol Chem. 2006 Dec 1;281(48):36552-9. doi: 10.1074/jbc.M606839200. Epub 2006 Sep 28. PMID: 17008312.

Dela Cruz R, Jeong MY, Winge DR. Cox1 mutation abrogates need for Cox23 in cytochrome c oxidase biogenesis. Microb Cell. 2016 Jun 30;3(7):275-284. doi: 10.15698/mic2016.07.511. PMID: 28357365; PMCID: PMC5354592.

Dickinson Q, Aufschnaiter A, Ott M, Meyer JG. Multi-omic integration by machine learning (MIMaL). Bioinformatics. 2022 Oct 31;38(21):4908-4918. doi: 10.1093/bioinformatics/btac631. Erratum in: Bioinformatics. 2023 Apr 3;39(4): PMID: 36106996; PMCID: PMC9801967.

Elliott LE, Saracco SA, Fox TD. Multiple roles of the Cox20 chaperone in assembly of Saccharomyces cerevisiae cytochrome c oxidase. Genetics. 2012 Feb;190(2):559-67. doi: 10.1534/genetics.111.135665. Epub 2011 Nov 17. PMID: 22095077; PMCID: PMC3276622.

Fiori A, Perez-Martinez X, Fox TD. Overexpression of the COX2 translational activator, Pet111p, prevents translation of COX1 mRNA and cytochrome c oxidase assembly in mitochondria of Saccharomyces cerevisiae. Mol Microbiol. 2005 Jun;56(6):1689-704. doi: 10.1111/j.1365-2958.2005.04658.x. PMID: 15916616.

Fiumera HL, Broadley SA, Fox TD. Translocation of mitochondrially synthesized Cox2 domains from the matrix to the intermembrane space. Mol Cell Biol. 2007 Jul;27(13):4664-

73. doi: 10.1128/MCB.01955-06. Epub 2007 Apr 23. PMID: 17452441; PMCID: PMC1951498.

Fox TD. Mitochondrial protein synthesis, import, and assembly. Genetics. 2012 Dec;192(4):1203-34. doi: 10.1534/genetics.112.141267. PMID: 23212899; PMCID: PMC3512135.

Fra A, Yoboue ED, Sitia R. Cysteines as Redox Molecular Switches and Targets of Disease. Front Mol Neurosci. 2017 Jun 6;10:167. doi: 10.3389/fnmol.2017.00167. PMID: 28634440; PMCID: PMC5459893.

Franco LVR, Moda BS, Soares MAKM, Barros MH. Msc6p is required for mitochondrial translation initiation in the absence of formylated Met-tRNAfMet. FEBS J. 2019 Apr;286(7):1407-1419. doi: 10.1111/febs.14785. Epub 2019 Mar 1. PMID: 30767393.

Franco LVR, Su CH, McStay GP, Yu GJ, Tzagoloff A. Cox2p of yeast cytochrome oxidase assembles as a stand-alone subunit with the Cox1p and Cox3p modules. J Biol Chem. 2018 Oct 26;293(43):16899-16911. doi: 10.1074/jbc.RA118.004138. Epub 2018 Sep 17. PMID: 30224355; PMCID: PMC6204888.

Franco LVR, Su CH, Tzagoloff A. Modular assembly of yeast mitochondrial ATP synthase and cytochrome oxidase. Biol Chem. 2020 May 26;401(6-7):835-853. doi: 10.1515/hsz-2020-0112. PMID: 32142477.

Fiumera HL, Broadley SA, Fox TD. Translocation of mitochondrially synthesized Cox2 domains from the matrix to the intermembrane space. Mol Cell Biol. 2007 Jul;27(13):4664-73. doi: 10.1128/MCB.01955-06. Epub 2007 Apr 23. PMID: 17452441; PMCID: PMC1951498.

Fiumera HL, Dunham MJ, Saracco SA, Butler CA, Kelly JA, Fox TD. Translocation and assembly of mitochondrially coded Saccharomyces cerevisiae cytochrome c oxidase subunit Cox2 by Oxa1 and Yme1 in the absence of Cox18. Genetics. 2009 Jun;182(2):519-28. doi: 10.1534/genetics.109.101196. Epub 2009 Mar 23. PMID: 19307606; PMCID: PMC2691760.

Fransen M, Lismont C, Walton P. The Peroxisome-Mitochondria Connection: How and Why? Int J Mol Sci. 2017 May 24;18(6):1126. doi: 10.3390/ijms18061126. PMID: 28538669; PMCID: PMC5485950.

Gaisne M, Bécam AM, Verdière J, Herbert CJ. A 'natural' mutation in Saccharomyces cerevisiae strains derived from S288c affects the complex regulatory gene HAP1 (CYP1). Curr Genet. 1999 Oct;36(4):195-200. doi: 10.1007/s002940050490. PMID: 10541856.

Gancedo C, Flores CL. Moonlighting proteins in yeasts. Microbiol Mol Biol Rev. 2008 Mar;72(1):197-210, table of contents. doi: 10.1128/MMBR.00036-07. PMID: 18322039; PMCID: PMC2268286.

Geldon S, Fernández-Vizarra E, Tokatlidis K. Redox-Mediated Regulation of Mitochondrial Biogenesis, Dynamics, and Respiratory Chain Assembly in Yeast and Human Cells. Front Cell Dev Biol. 2021 Sep 7;9:720656. doi: 10.3389/fcell.2021.720656. PMID: 34557489; PMCID: PMC8452992.

Ghosh A, Pratt AT, Soma S, Theriault SG, Griffin AT, Trivedi PP, Gohil VM. Mitochondrial disease genes COA6, COX6B and SCO2 have overlapping roles in COX2 biogenesis. Hum Mol Genet. 2016 Feb 15;25(4):660-71. doi: 10.1093/hmg/ddv503. Epub 2015 Dec 15. PMID: 26669719; PMCID: PMC4743686.

Glerum DM, Shtanko A, Tzagoloff A. SCO1 and SCO2 act as high copy suppressors of a mitochondrial copper recruitment defect in Saccharomyces cerevisiae. J Biol Chem. 1996a Aug 23;271(34):20531-5. doi: 10.1074/jbc.271.34.20531. PMID: 8702795.

Glerum DM, Shtanko A, Tzagoloff A. Characterization of COX17, a yeast gene involved in copper metabolism and assembly of cytochrome oxidase. J Biol Chem. 1996b Jun 14;271(24):14504-9. doi: 10.1074/jbc.271.24.14504. PMID: 8662933.

Goffeau A, Barrell BG, Bussey H, Davis RW, Dujon B, Feldmann H, Galibert F, Hoheisel JD, Jacq C, Johnston M, Louis EJ, Mewes HW, Murakami Y, Philippsen P, Tettelin H, Oliver SG. Life with 6000 genes. Science. 1996 Oct 25;274(5287):546, 563-7. doi: 10.1126/science.274.5287.546. PMID: 8849441.

Gomes F, Palma FR, Barros MH, Tsuchida ET, Turano HG, Alegria TGP, Demasi M, Netto LES. Proteolytic cleavage by the inner membrane peptidase (IMP) complex or Oct1 peptidase controls the localization of the yeast peroxiredoxin Prx1 to distinct mitochondrial compartments. J Biol Chem. 2017 Oct 13;292(41):17011-17024. doi: 10.1074/jbc.M117.788588. Epub 2017 Aug 18. PMID: 28821623; PMCID: PMC5641892.

Gomes F, Tahara EB, Busso C, Kowaltowski AJ, Barros MH. nde1 deletion improves mitochondrial DNA maintenance in Saccharomyces cerevisiae coenzyme Q mutants. Biochem J. 2013 Feb 1;449(3):595-603. doi: 10.1042/BJ20121432. PMID: 23116202.

Grant CM, MacIver FH, Dawes IW. Glutathione is an essential metabolite required for resistance to oxidative stress in the yeast Saccharomyces cerevisiae. Curr Genet. 1996 May;29(6):511-5. doi: 10.1007/BF02426954. PMID: 8662189.

Green-Willms NS, Butler CA, Dunstan HM, Fox TD. Pet111p, an inner membrane-bound translational activator that limits expression of the Saccharomyces cerevisiae

mitochondrial gene COX2. J Biol Chem. 2001 Mar 2;276(9):6392-7. doi: 10.1074/jbc.M009856200. Epub 2000 Dec 5. PMID: 11106667.

Hanschmann EM, Godoy JR, Berndt C, Hudemann C, Lillig CH. Thioredoxins, glutaredoxins, and peroxiredoxins--molecular mechanisms and health significance: from cofactors to antioxidants to redox signaling. Antioxid Redox Signal. 2013 Nov 1;19(13):1539-605. doi: 10.1089/ars.2012.4599. Epub 2013 Mar 28. PMID: 23397885; PMCID: PMC3797455.

Hanson GT, Aggeler R, Oglesbee D, Cannon M, Capaldi RA, Tsien RY, Remington SJ. Investigating mitochondrial redox potential with redox-sensitive green fluorescent protein indicators. J Biol Chem. 2004 Mar 26;279(13):13044-53. doi: 10.1074/jbc.M312846200. Epub 2004 Jan 13. PMID: 14722062.

He S, Fox TD. Membrane translocation of mitochondrially coded Cox2p: distinct requirements for export of N and C termini and dependence on the conserved protein Oxa1p. Mol Biol Cell. 1997 Aug;8(8):1449-60. doi: 10.1091/mbc.8.8.1449. PMID: 9285818; PMCID: PMC276169.

He S, Fox TD. Mutations affecting a yeast mitochondrial inner membrane protein, pnt1p, block export of a mitochondrially synthesized fusion protein from the matrix. Mol Cell Biol. 1999 Oct;19(10):6598-607. doi: 10.1128/MCB.19.10.6598. PMID: 10490599; PMCID: PMC84629.

Hell K, Herrmann J, Pratje E, Neupert W, Stuart RA. Oxa1p mediates the export of the N- and C-termini of pCoxII from the mitochondrial matrix to the intermembrane space. FEBS Lett. 1997 Dec 1;418(3):367-70. doi: 10.1016/s0014-5793(97)01412-9. PMID: 9428747.

Hell K, Tzagoloff A, Neupert W, Stuart RA. Identification of Cox20p, a novel protein involved in the maturation and assembly of cytochrome oxidase subunit 2. J Biol Chem. 2000 Feb 18;275(7):4571-8. doi: 10.1074/jbc.275.7.4571. PMID: 10671482.

Herrmann, J. M., Foelsch, H., Neupert, W., and Stuart, R. A. (1994) Isolation of yeast mitochondria and study of mitochondrial protein translation. In: Celis, J. R., ed. Cell Biology, Laboratory Handbook Vol. I, Academic Press, San Diego: 538–544

Hill JE, Myers AM, Koerner TJ, Tzagoloff A. Yeast/E. coli shuttle vectors with multiple unique restriction sites. Yeast. 1986 Sep;2(3):163-7. doi: 10.1002/yea.320020304. PMID: 3333305.

Horlbeck MA, Xu A, Wang M, Bennett NK, Park CY, Bogdanoff D, Adamson B, Chow ED, Kampmann M, Peterson TR, Nakamura K, Fischbach MA, Weissman JS, Gilbert LA. Mapping the Genetic Landscape of Human Cells. Cell. 2018 Aug 9;174(4):953-967.e22. doi: 10.1016/j.cell.2018.06.010. Epub 2018 Jul 19. PMID: 30033366; PMCID: PMC6426455.

Jeffery CJ. Protein moonlighting: what is it, and why is it important? Philos Trans R Soc Lond B Biol Sci. 2018 Jan 19;373(1738):20160523. doi: 10.1098/rstb.2016.0523. PMID: 29203708; PMCID: PMC5717523.

Jett KA, Leary SC. Building the CuA site of cytochrome c oxidase: A complicated, redox-dependent process driven by a surprisingly large complement of accessory proteins. J Biol Chem. 2018 Mar 30;293(13):4644-4652. doi: 10.1074/jbc.R117.816132. Epub 2017 Sep 29. PMID: 28972150; PMCID: PMC5880131.

Kaur J, Stuart RA. Truncation of the Mrp20 protein reveals new ribosome-assembly subcomplex in mitochondria. EMBO Rep. 2011 Sep 1;12(9):950-5. doi: 10.1038/embor.2011.133. PMID: 21779004; PMCID: PMC3166459.

Keerthiraju E, Du C, Tucker G, Greetham D. A Role for COX20 in Tolerance to Oxidative Stress and Programmed Cell Death in Saccharomyces cerevisiae. Microorganisms. 2019 Nov 18;7(11):575. doi: 10.3390/microorganisms7110575. PMID: 31752220; PMCID: PMC6920987.

Khalimonchuk O, Bird A, Winge DR. Evidence for a pro-oxidant intermediate in the assembly of cytochrome oxidase. J Biol Chem. 2007 Jun 15;282(24):17442-9

Kwolek-Mirek M, Bartosz G, Spickett CM. Sensitivity of antioxidant-deficient yeast to hypochlorite and chlorite. Yeast. 2011 Aug;28(8):595-609. doi: 10.1002/yea.1889. Epub 2011 Jul 14. PMID: 21761455.

Laemmli UK. Cleavage of structural proteins during the assembly of the head of bacteriophage T4. Nature. 1970 Aug 15;227(5259):680-5. doi: 10.1038/227680a0. PMID: 5432063.

Leary SC, Cobine PA, Kaufman BA, Guercin GH, Mattman A, Palaty J, Lockitch G, Winge DR, Rustin P, Horvath R, Shoubridge EA. The human cytochrome c oxidase assembly factors SCO1 and SCO2 have regulatory roles in the maintenance of cellular copper homeostasis. Cell Metab. 2007 Jan;5(1):9-20. doi: 10.1016/j.cmet.2006.12.001. Erratum in: Cell Metab. 2007 May;5(5):403. PMID: 17189203.

Lorenzi I, Oeljeklaus S, Ronsör C, Bareth B, Warscheid B, Rehling P, Dennerlein S. Ribosome-Associated Mba1 Escorts Cox2 from Insertion Machinery to Maturing Assembly Intermediates. Mol Cell Biol. 2016 Oct 28;36(22):2782-2793. doi: 10.1128/MCB.00361-16. PMID: 27550809; PMCID: PMC5086520.

Longen S, Bien M, Bihlmaier K, Kloeppel C, Kauff F, Hammermeister M, Westermann B, Herrmann JM, Riemer J. Systematic analysis of the twin cx(9)c protein family. J Mol

Biol. 2009 Oct 23;393(2):356-68. doi: 10.1016/j.jmb.2009.08.041. Epub 2009 Aug 21. PMID: 19703468.

Lowry OH, Rosebrough NJ, Farr AL, Randall RJ. Protein measurement with the Folin phenol reagent. J Biol Chem. 1951 Nov;193(1):265-75. PMID: 14907713.

Mesecke N, Terziyska N, Kozany C, Baumann F, Neupert W, Hell K, Herrmann JM. A disulfide relay system in the intermembrane space of mitochondria that mediates protein import. Cell. 2005 Jul 1;121(7):1059-69. doi: 10.1016/j.cell.2005.04.011. PMID: 15989955.

Morgan B, Sobotta MC, Dick TP. Measuring E(GSH) and H2O2 with roGFP2-based redox probes. Free Radic Biol Med. 2011 Dec 1;51(11):1943-51. doi: 10.1016/j.freeradbiomed.2011.08.035. Epub 2011 Sep 10. PMID: 21964034.

Mulero JJ, Fox TD. PET111 acts in the 5'-leader of the Saccharomyces cerevisiae mitochondrial COX2 mRNA to promote its translation. Genetics. 1993 Mar;133(3):509-16. doi: 10.1093/genetics/133.3.509. PMID: 7681022; PMCID: PMC1205339.

Mumberg D, Müller R, Funk M. Yeast vectors for the controlled expression of heterologous proteins in different genetic backgrounds. Gene. 1995 Apr 14;156(1):119-22. doi: 10.1016/0378-1119(95)00037-7. PMID: 7737504.

Nobrega MP, Bandeira SC, Beers J, Tzagoloff A. Characterization of COX19, a widely distributed gene required for expression of mitochondrial cytochrome oxidase. J Biol Chem. 2002 Oct 25;277(43):40206-11. doi: 10.1074/jbc.M207348200. Epub 2002 Aug 8. PMID: 12171940.

Nunnari J, Fox TD, Walter P. A mitochondrial protease with two catalytic subunits of nonoverlapping specificities. Science. 1993 Dec 24;262(5142):1997-2004. doi: 10.1126/science.8266095. PMID: 8266095.

Nývltová E, Dietz JV, Seravalli J, Khalimonchuk O, Barrientos A. Coordination of metal center biogenesis in human cytochrome c oxidase. Nat Commun. 2022 Jun 24;13(1):3615. doi: 10.1038/s41467-022-31413-1. PMID: 35750769; PMCID: PMC9232578.

Peleh V, Cordat E, Herrmann JM. Mia40 is a trans-site receptor that drives protein import into the mitochondrial intermembrane space by hydrophobic substrate binding. Elife. 2016 Jun 25;5:e16177. doi: 10.7554/eLife.16177. PMID: 27343349; PMCID: PMC4951193.

Peña-Castillo L, Hughes TR. Why are there still over 1000 uncharacterized yeast genes? Genetics. 2007 May;176(1):7-14. doi: 10.1534/genetics.107.074468. Epub 2007 Apr 15. PMID: 17435240; PMCID: PMC1893027.

Reinders J, Wagner K, Zahedi RP, Stojanovski D, Eyrich B, van der Laan M, Rehling P, Sickmann A, Pfanner N, Meisinger C. Profiling phosphoproteins of yeast mitochondria reveals a role of phosphorylation in assembly of the ATP synthase. Mol Cell Proteomics. 2007 Nov;6(11):1896-906. doi: 10.1074/mcp.M700098-MCP200. Epub 2007 Aug 29. PMID: 17761666.

Reinders J, Zahedi RP, Pfanner N, Meisinger C, Sickmann A. Toward the complete yeast mitochondrial proteome: multidimensional separation techniques for mitochondrial proteomics. J Proteome Res. 2006 Jul;5(7):1543-54. doi: 10.1021/pr050477f. PMID: 16823961.

Repetto B, Tzagoloff A. Structure and regulation of KGD2, the structural gene for yeast dihydrolipoyl transsuccinylase. Mol Cell Biol. 1990 Aug;10(8):4221-32. doi: 10.1128/mcb.10.8.4221-4232.1990. PMID: 2115121; PMCID: PMC360958.

Santos B, Zeng R, Jorge SF, Ferreira-Junior JR, Barrientos A, Barros MH. Functional analyses of mitoribosome 54S subunit devoid of mitochondria-specific protein sequences. Yeast. 2022 Mar;39(3):208-229. doi: 10.1002/yea.3678. Epub 2021 Nov 10. PMID: 34713496; PMCID: PMC8969203.

Saracco SA, Fox TD. Cox18p is required for export of the mitochondrially encoded Saccharomyces cerevisiae Cox2p C-tail and interacts with Pnt1p and Mss2p in the inner membrane. Mol Biol Cell. 2002 Apr;13(4):1122-31. doi: 10.1091/mbc.01-12-0580. PMID: 11950926; PMCID: PMC102256.

Schägger H, Pfeiffer K. Supercomplexes in the respiratory chains of yeast and mammalian mitochondria. EMBO J. 2000 Apr 17;19(8):1777-83. doi: 10.1093/emboj/19.8.1777. PMID: 10775262; PMCID: PMC302020.

Souza RL, Green-Willms NS, Fox TD, Tzagoloff A, Nobrega FG. Cloning and characterization of COX18, a Saccharomyces cerevisiae PET gene required for the assembly of cytochrome oxidase. J Biol Chem. 2000 May 19;275(20):14898-902. doi: 10.1074/jbc.275.20.14898. PMID: 10809734.

Su CH, Tzagoloff A. Cox16 protein is physically associated with Cox1p assembly intermediates and with cytochrome oxidase. J Biol Chem. 2017 Sep 29;292(39):16277-16283. doi: 10.1074/jbc.M117.801811. Epub 2017 Aug 16. PMID: 28821616; PMCID: PMC5625057.

Sung AY, Floyd BJ, Pagliarini DJ. Systems Biochemistry Approaches to Defining Mitochondrial Protein Function. Cell Metab. 2020 Apr 7;31(4):669-678. doi: 10.1016/j.cmet.2020.03.011. PMID: 32268114; PMCID: PMC7176052.

Stefely JA, Kwiecien NW, Freiberger EC, Richards AL, Jochem A, Rush MJP, Ulbrich A, Robinson KP, Hutchins PD, Veling MT, Guo X, Kemmerer ZA, Connors KJ, Trujillo

EA, Sokol J, Marx H, Westphall MS, Hebert AS, Pagliarini DJ, Coon JJ. Mitochondrial protein functions elucidated by multi-omic mass spectrometry profiling. Nat Biotechnol. 2016 Nov;34(11):1191-1197. doi: 10.1038/nbt.3683. Epub 2016 Sep 26. PMID: 27669165; PMCID: PMC5101133.

Stroud DA, Surgenor EE, Formosa LE, Reljic B, Frazier AE, Dibley MG, Osellame LD, Stait T, Beilharz TH, Thorburn DR, Salim A, Ryan MT. Accessory subunits are integral for assembly and function of human mitochondrial complex I. Nature. 2016 Oct 6;538(7623):123-126. doi: 10.1038/nature19754. Epub 2016 Sep 14. PMID: 27626371.

Tzagoloff A, Akai A, Needleman RB. Assembly of the mitochondrial membrane system: isolation of nuclear and cytoplasmic mutants of Saccharomyces cerevisiae with specific defects in mitochondrial functions. J Bacteriol. 1975 Jun;122(3):826-31. doi: 10.1128/jb.122.3.826-831.1975. PMID: 168180; PMCID: PMC246131.

Usaj M, Tan Y, Wang W, VanderSluis B, Zou A, Myers CL, Costanzo M, Andrews B, Boone C. TheCellMap.org: A Web-Accessible Database for Visualizing and Mining the Global Yeast Genetic Interaction Network. G3 (Bethesda). 2017 May 5;7(5):1539-1549. doi: 10.1534/g3.117.040220. PMID: 28325812; PMCID: PMC5427489.

Veenhuis M, Mateblowski M, Kunau WH, Harder W. Proliferation of microbodies in Saccharomyces cerevisiae. Yeast. 1987 Jun;3(2):77-84. doi: 10.1002/yea.320030204. PMID: 3332968.

Veniamin S, Sawatzky LG, Banting GS, Glerum DM. Characterization of the peroxide sensitivity of COX-deficient yeast strains reveals unexpected relationships between COX assembly proteins. Free Radic Biol Med. 2011 Oct 15;51(8):1589-600. doi: 10.1016/j.freeradbiomed.2011.06.024. Epub 2011 Jul 23. PMID: 21821119.

West JD, Roston TJ, David JB, Allan KM, Loberg MA. Piecing Together How Peroxiredoxins Maintain Genomic Stability. Antioxidants (Basel). 2018 Nov 28;7(12):177. doi: 10.3390/antiox7120177. PMID: 30486489; PMCID: PMC6316004.

Wood V, Lock A, Harris MA, Rutherford K, Bähler J, Oliver SG. Hidden in plain sight: what remains to be discovered in the eukaryotic proteome? Open Biol. 2019 Feb 28;9(2):180241. doi: 10.1098/rsob.180241. PMID: 30938578; PMCID: PMC6395881.

Yifrach E, Holbrook-Smith D, Bürgi J, Othman A, Eisenstein M, van Roermund CW, Visser W, Tirosh A, Rudowitz M, Bibi C, Galor S, Weill U, Fadel A, Peleg Y, Erdmann R, Waterham HR, Wanders RJA, Wilmanns M, Zamboni N, Schuldiner M, Zalckvar E. Systematic multi-level analysis of an organelle proteome reveals new peroxisomal functions. Mol Syst Biol. 2022 Sep;18(9):e11186. doi: 10.15252/msb.202211186. PMID: 36164978; PMCID: PMC9513677.

Yost HJ, Lindquist S. Heat shock proteins affect RNA processing during the heat shock response of Saccharomyces cerevisiae. Mol Cell Biol. 1991 Feb;11(2):1062-8. doi: 10.1128/mcb.11.2.1062-1068.1991. PMID: 1899282; PMCID: PMC359779.

Zampol MA, Busso C, Gomes F, Ferreira-Junior JR, Tzagoloff A, Barros MH. Over-expression of COQ10 in Saccharomyces cerevisiae inhibits mitochondrial respiration. Biochem Biophys Res Commun. 2010 Nov 5;402(1):82-7. doi: 10.1016/j.bbrc.2010.09.118. Epub 2010 Oct 8. PMID: 20933507; PMCID: PMC3175363.

Table 1 – Yeast strains and relevant genotype used in this work.

Strain	Genotype	Reference
W303-1B	*MATα ade2-1 trp1-1 his3-1,15 leu2-3,112 ura3-1*	Rothstein, R.*
W303-1A	*MATa ade2-1 trp1-1 his3-1,15 leu2-3,112 ura3-1*	Rothstein, R.*
BY4742	*MATα his3Δ1 leu2Δ0 lys2Δ0 ura3Δ0*	Euroscarf
W303/GAL10-DMO2	MATα *ade2-1 trp1-1 his3-1,15 leu2-3,112 ura3-1 leu2::pIGAL-DMO2*	This study
W303/GPD-DMO2	MATα *ade2-1 trp1-1 his3-1,15 leu2-3,112 ura3-1 pCGPD-DMO2*	This study
W303/TEF-DMO2	MATα *ade2-1 trp1-1 his3-1,15 leu2-3,112 ura3-1 leu2::pITEF-DMO2*	This study
W303ΔDMO2-H	*MATa ade2-1 trp1-1 his3-1,15 leu2-3,112 ura3-1 dmo2::HIS3*	This study
W303ΔDMO2-L	*MATa ade2-1 trp1-1 his3-1,15 leu2-3,112 ura3-1 dmo2::LEU2*	This study
W303/DMO2-CH	*MATa ade2-1 trp1-1 his3-1,15 leu2-3,112 ura3-1 dmo2::HIS3 trp1::pIWDMO2-CH*	This study
W303/DMO2-HA	*MATaade2-1 trp1-1 his3-1,15 leu2-3,112 ura3-1 dmo2::HIS3 ura3::pIWDMO2-CH*	This study
W303/DMO2-ST12	*MATa ade2-1 trp1-1 his3-1,15 leu2-3,112 ura3-1 dmo2::HIS3 trp1::pIWDMO2-C24S*	This study
W303/DMO2-ST13	*MATa ade2-1 trp1-1 his3-1,15 leu2-3,112 ura3-1 dmo2::HIS3 trp1::pIWDMO2-C27S*	This study
W303/DMO2-ST14	*MATa ade2-1 trp1-1 his3-1,15 leu2-3,112 ura3-1 dmo2::HIS3 trp1::pIWDMO2-C24S-C27S*	This study
W303ΔCOX20	*MATα ade2-1 trp1-1 his3-1,15 leu2-3,112 ura3-1 cox20::URA3*	Hell et al., 2000
W303ΔSCO2	*MATa ade2-1 trp1-1 his3-1,15 leu2-3,112 ura3-1 sco2::kanMX*	This study
aW303ΔSCO2ΔCOX20	*MATa ade2-1 trp1-1 his3-1,15 leu2-3,112 ura3-1 sco2::kanmX cox20::URA3*	This study
W303ΔDMO2ΔCOX20	*MATa ade2-1 trp1-1 his3-1,15 leu2-3,112 ura3-1 dmo2::HIS3 cox20::URA3*	This study
W303ΔCOX18	*MATα ade2-1 trp1-1 his3-1,15 leu2-3,112 ura3-1 cox18::URA3*	Souza et al., 2000
W303ΔDMO2ΔCOX18	*MATa ade2-1 trp1-1 his3-1,15 leu2-3,112 ura3-1 dmo2::HIS3 cox18::URA3*	Souza et al., 2000

aW303 ΔCOX23	*MATa ade2-1 trp1-1 his3-1,15 leu2-3,112 ura3-1 cox23::HIS3*	Barros et al., 2004
BYΔCOX23	*MATα his3Δ1 leu2Δ0 lys2Δ0 ura3Δ0 cox23::kanMX*	Euroscarf
aW303ΔIMP2	*MATaade2-1 trp1-1 his3-1,15 leu2-3,112 ura3-1 imp2::URA3*	Barros et al., 2002
aW303ΔDMO2ΔIMP2	*MATa ade2-1 trp1-1 his3-1,15 leu2-3,112 ura3-1 dmo2::HIS3 imp2::URA3*	Souza et al., 2000
* R. Rothstein, Department of Human Genetics and Development, Columbia University.		